

Weldability of Creep-Resistant Alloys for Advanced Fossil Power Plants

Zhili Feng, Wei Zhang, Jason Wang, Yanli Wang, Yanfei Gao*

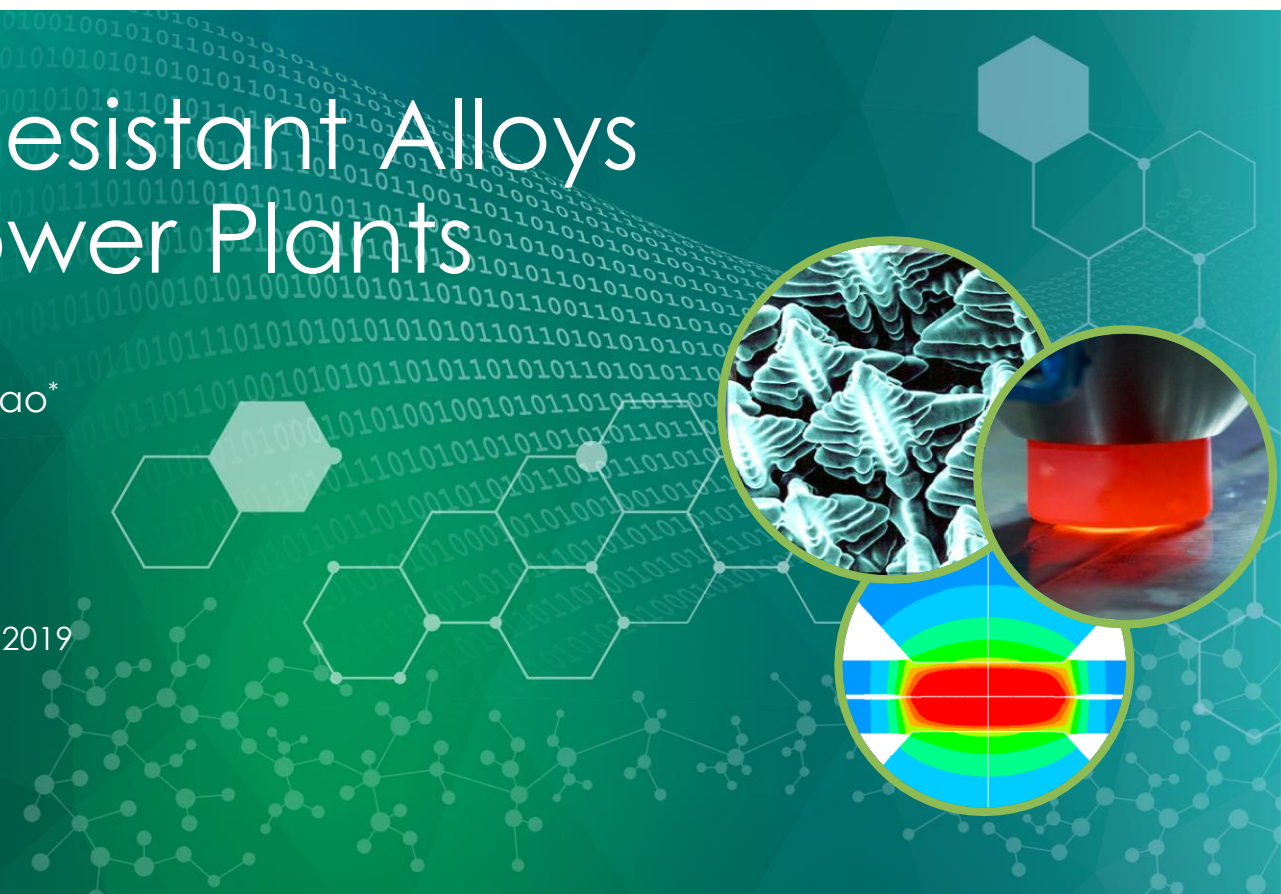
Oak Ridge National Laboratory

*University of Tennessee

2019 Project Review Meeting for Crosscutting Research, April 9-11, 2019

Program Manager: Vito Cedro III

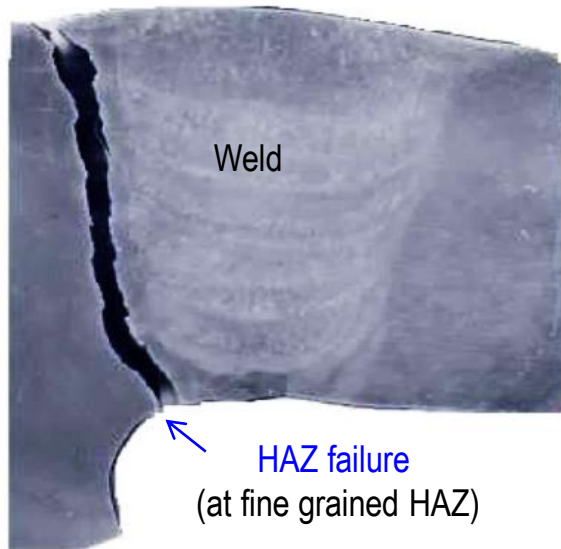
fengz@ornl.gov



Background: Weld can be the weakest link

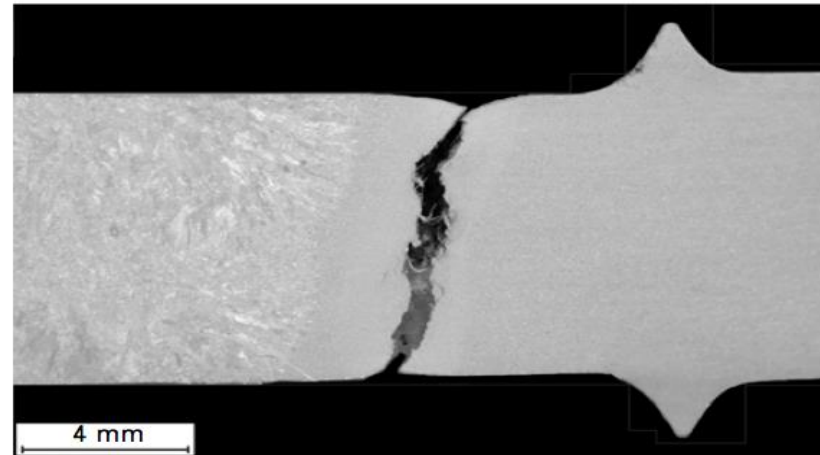
- Weldability issues (aka Type IV cracking) in Creep Strength Enhanced Ferritic Steels weldments

HAZ cracking in a 9-12Cr steel

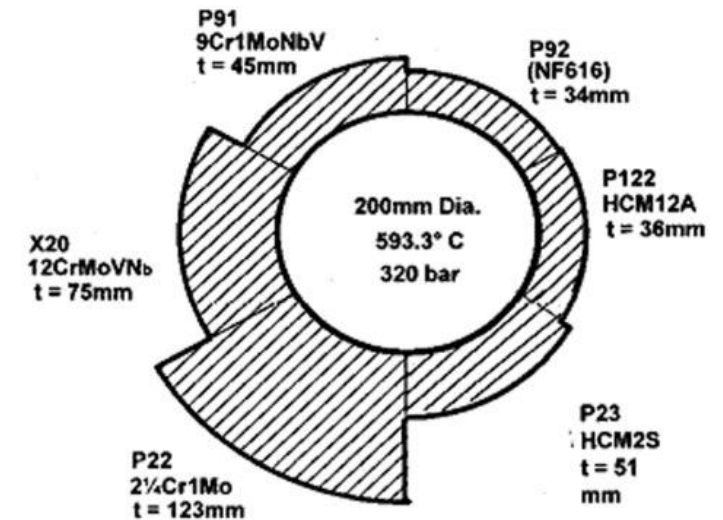


Source: ETD Ltd.

Type IV failure of E911 pipe weldment



Abe, F., Kern, T.U. and Viswanathan, R. 2008

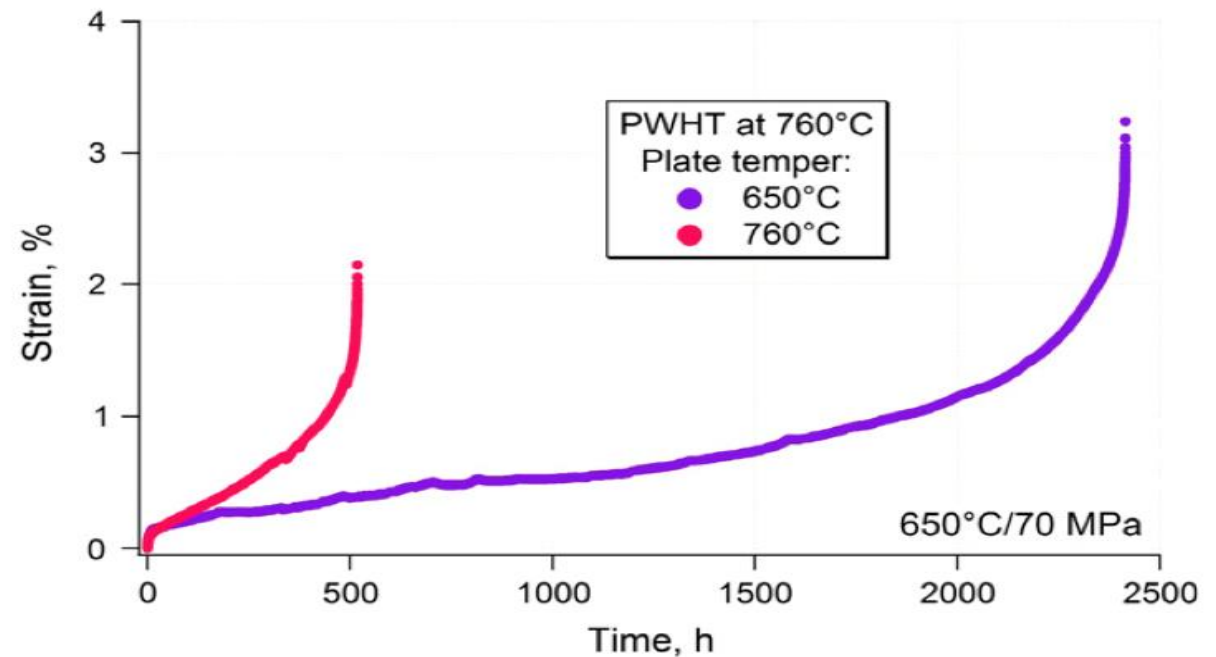
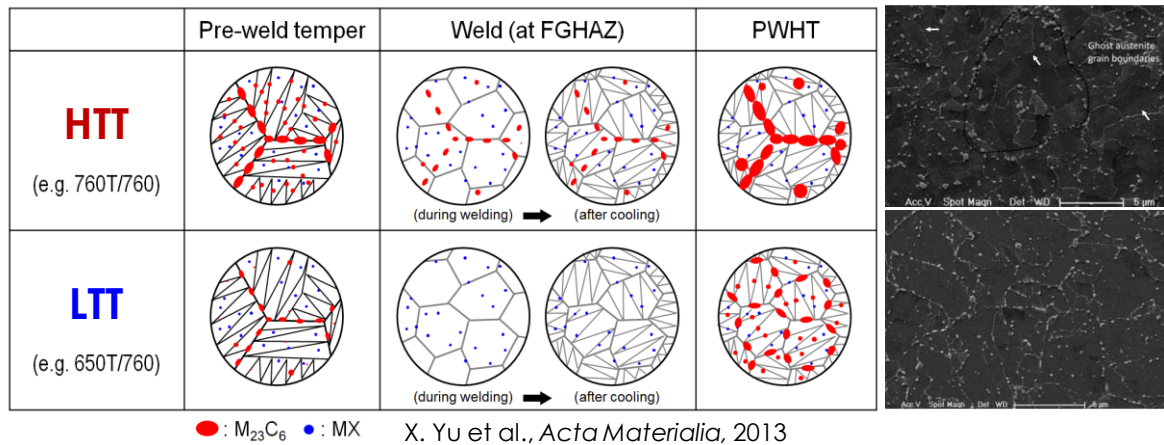


- Major reduction in creep strength in the weld region can be as high as 50% of base metal. Effectively negate the benefit of higher creep resistance steels such as P91, P92 etc.
- Lack of reliable predictive modeling tool makes it difficult to effectively incorporate welding technology innovations for creep resistance improvement in design and service. Life assessment of existing power plant and scheduling maintenance and repair

Degradation of Creep Performance in CSEF Weld

- Not all welds are created equal – it is possible to alter microstructure to improve creep performance of welds
- Weld creep performance assessment tool needs to include microstructure variations and associated different creep deformation/failure mechanisms so that innovations in weld creep performance improvement can be practiced with high confidence

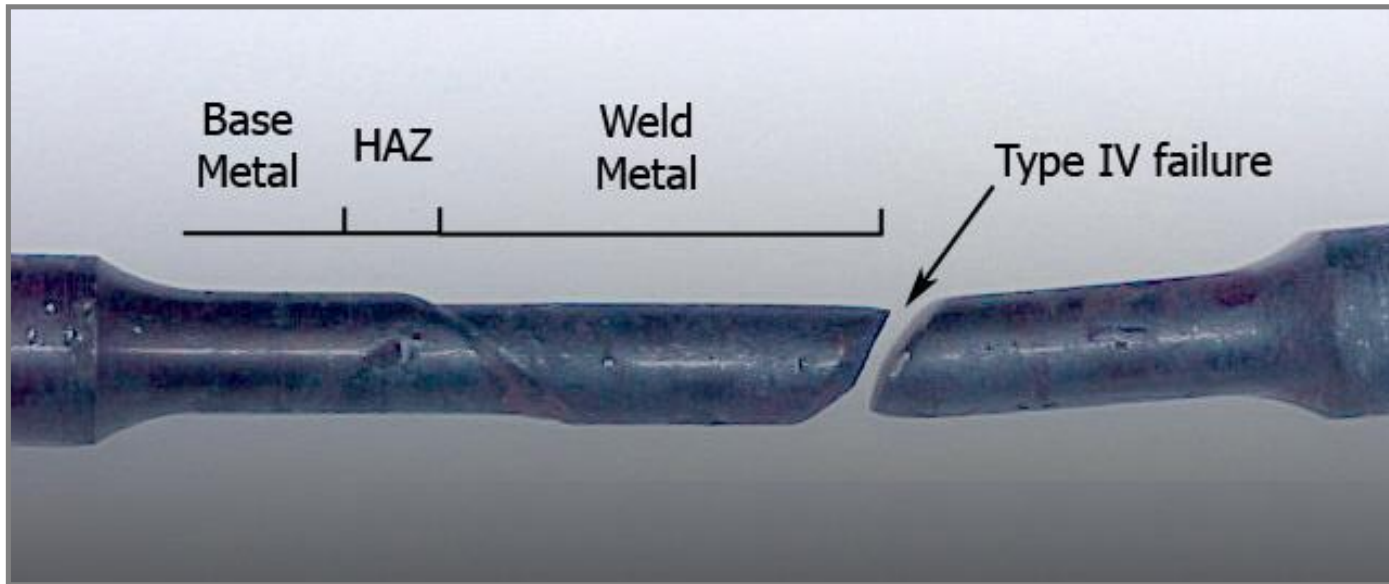
Table: Microstructure evolution at fine grain heat affected zone



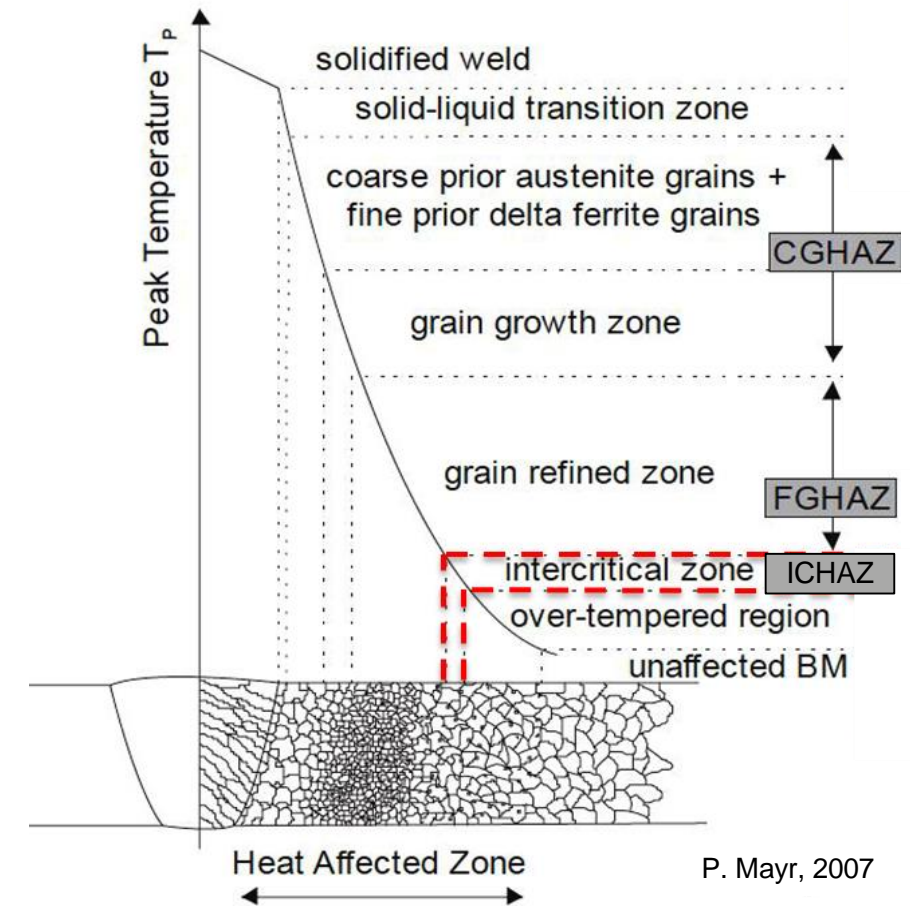
Project Goal and Scope

- Develop an Integrated Computational Welding Engineering modeling (ICWE) tool for creep deformation and failure in welded structures of Creep Strength Enhanced Ferritic (CSEF) Steels
- Develop a new creep test approach with purposely built system suitable to determine the highly nonuniform creep deformation and failure in the a weldment to validate and refine the model
- Two levels of modeling frameworks have been under development
 - An engineering approach for weld creep performance based on experimental data (Level 1 model)
 - Microstructure informed ICWE model for CSEF steels weld creep performance prediction (Level 2 model)

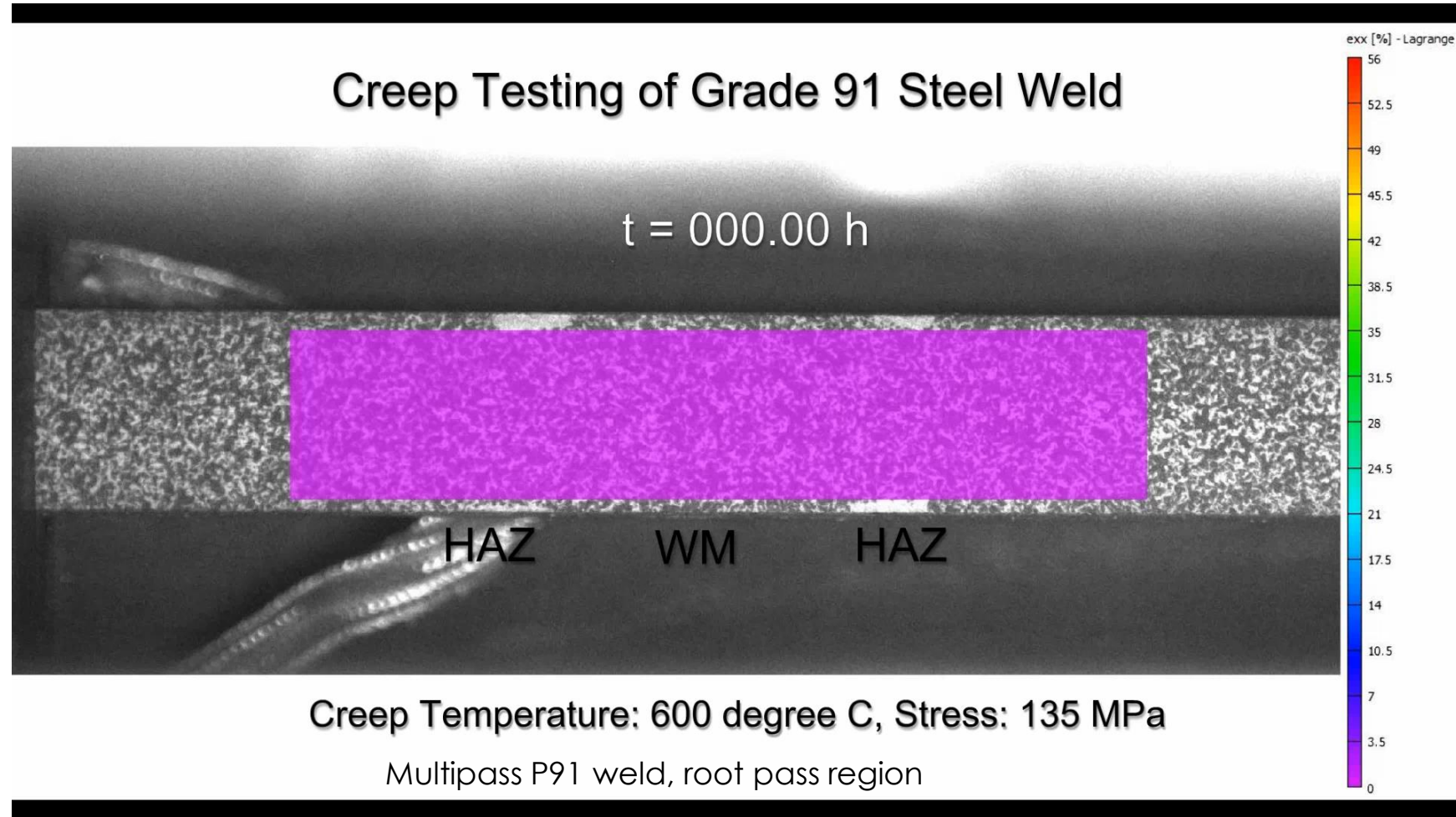
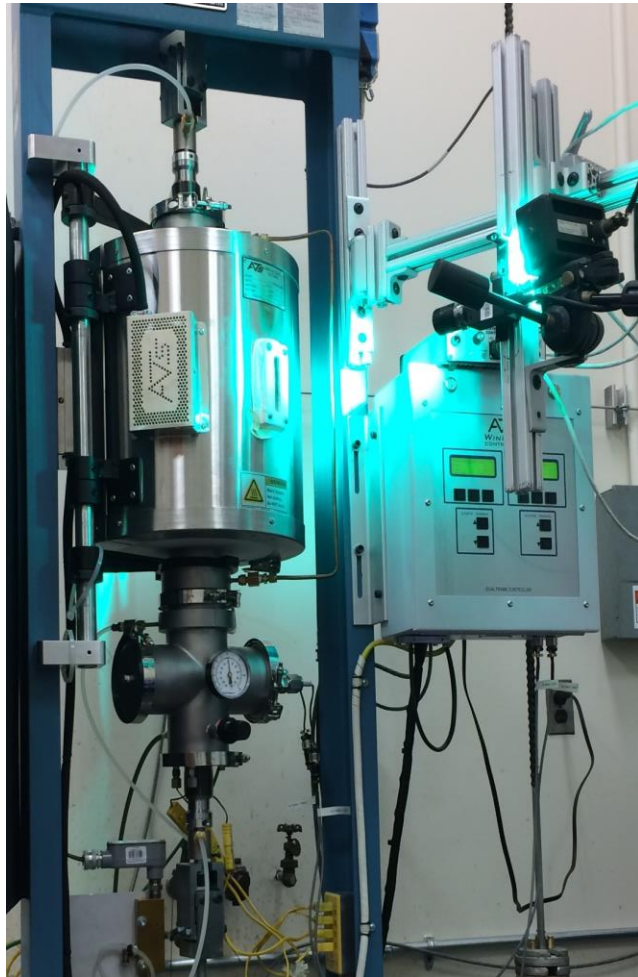
What's the local creep behavior in HAZ that controls Type IV cracking in Grade 91 welds?



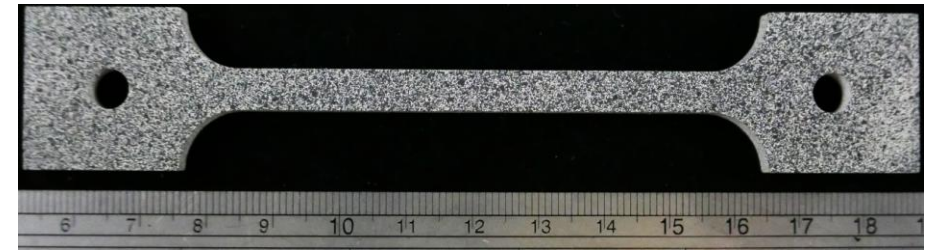
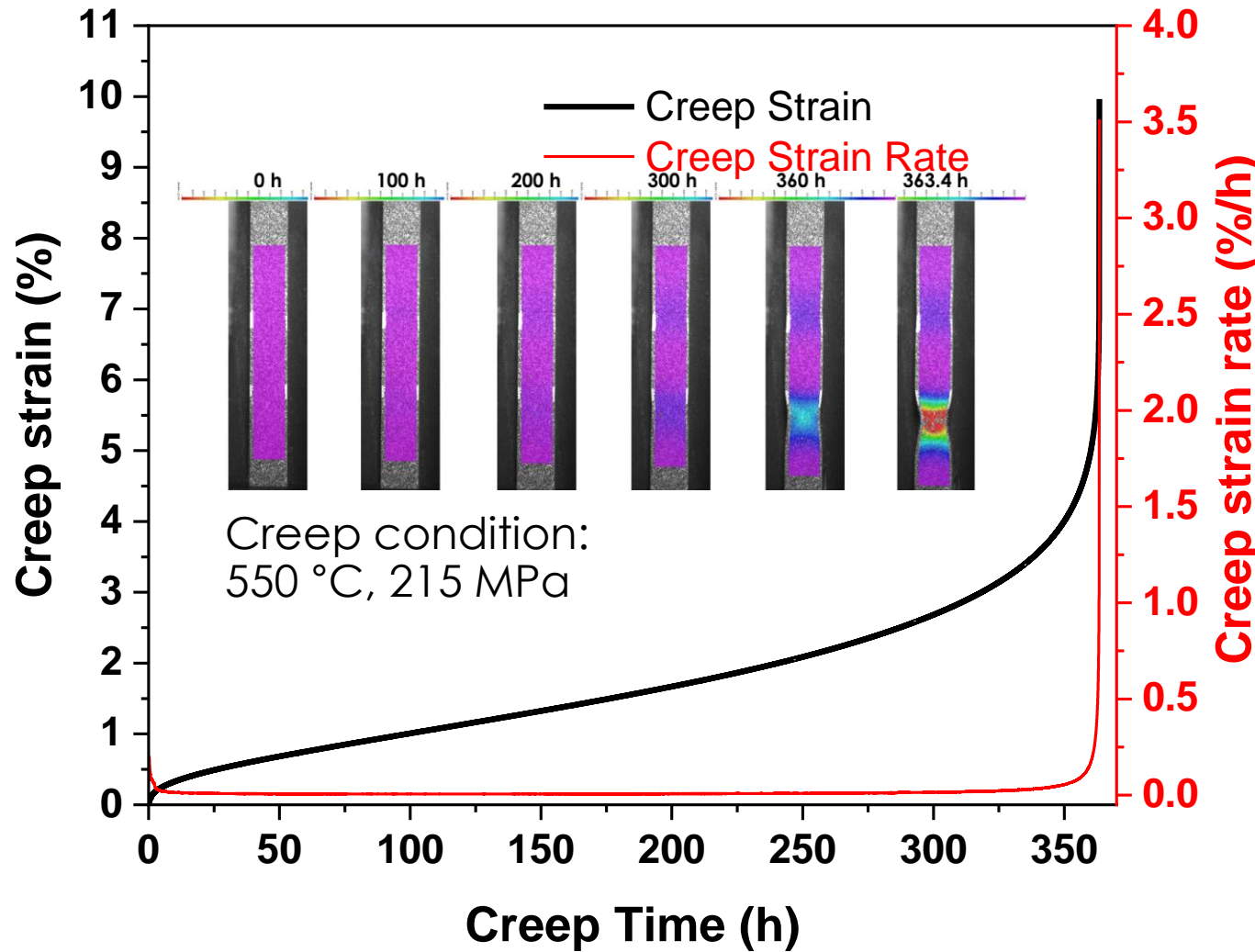
- Cracking occurs in a very narrow region, typically ~1 mm wide
- Measurement needs to have sub-mm spatial resolution
- Standard creep test (for base metal) cannot capture such highly localized creep deformation



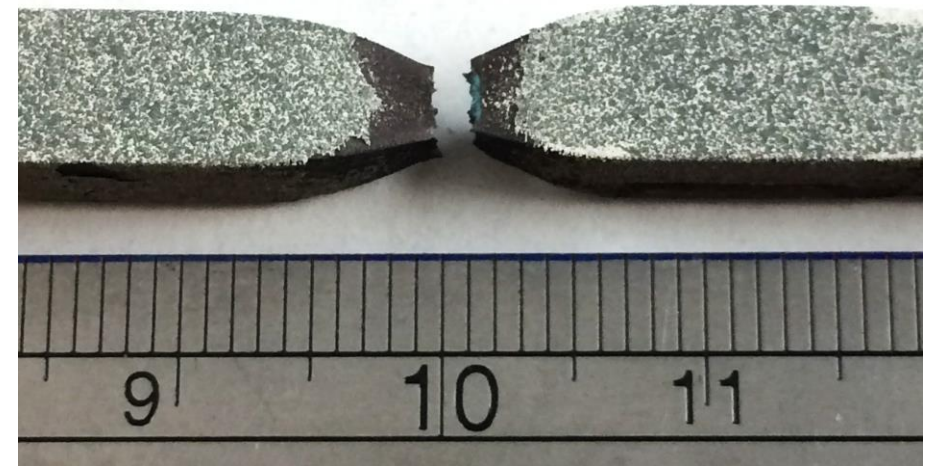
A purposely built in-situ full-field creep strain measurement system with high temperature DIC



Creep measurement using "standard" extensometer shows very low creep strain before ternary creep leading to failure

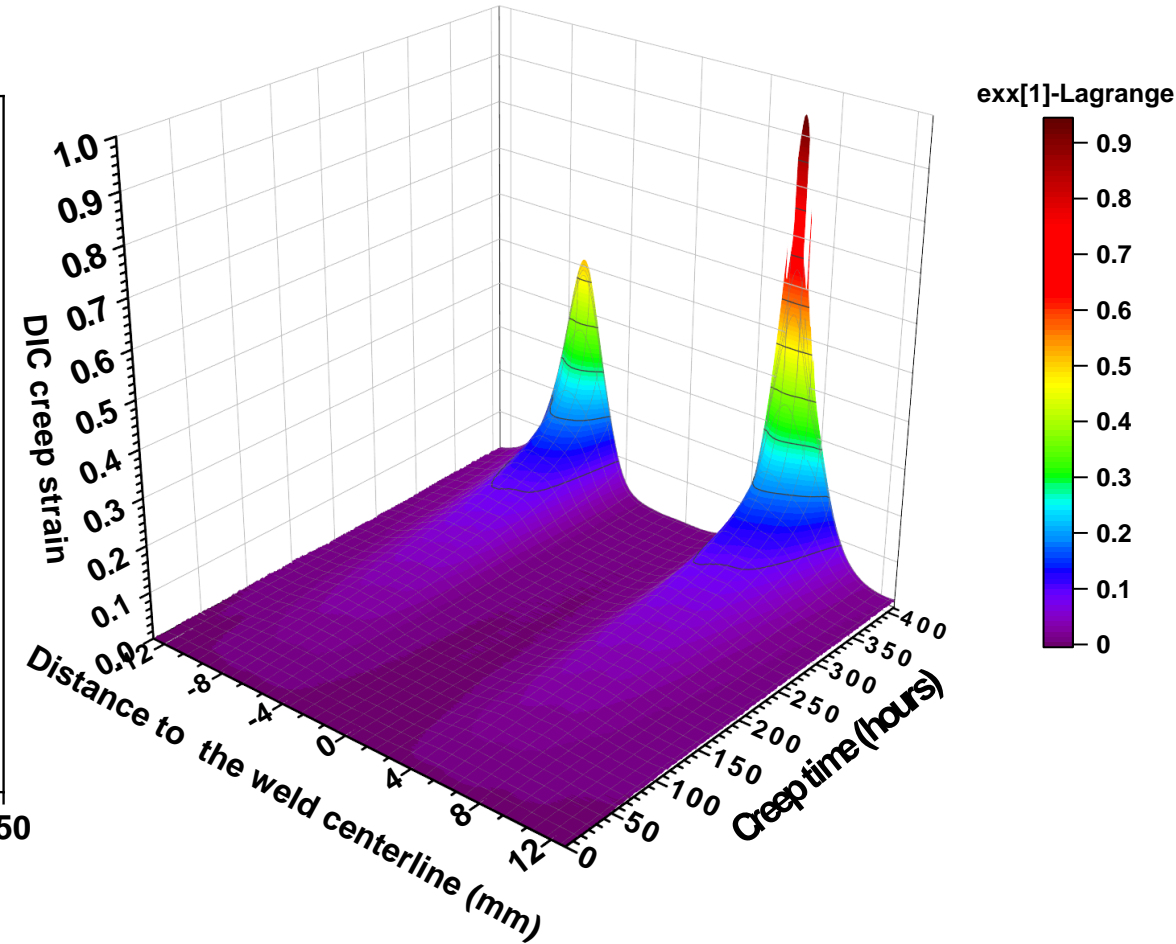
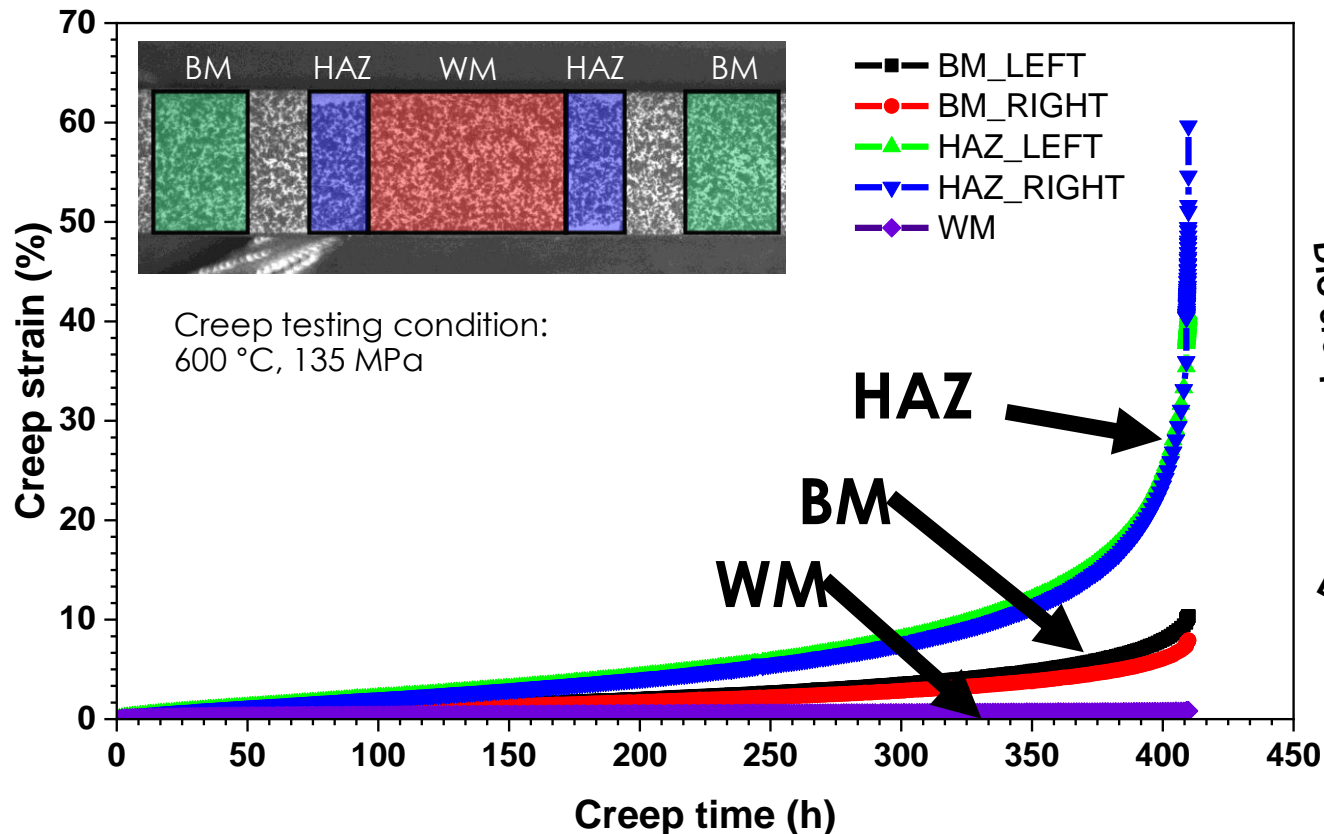


Before creep testing



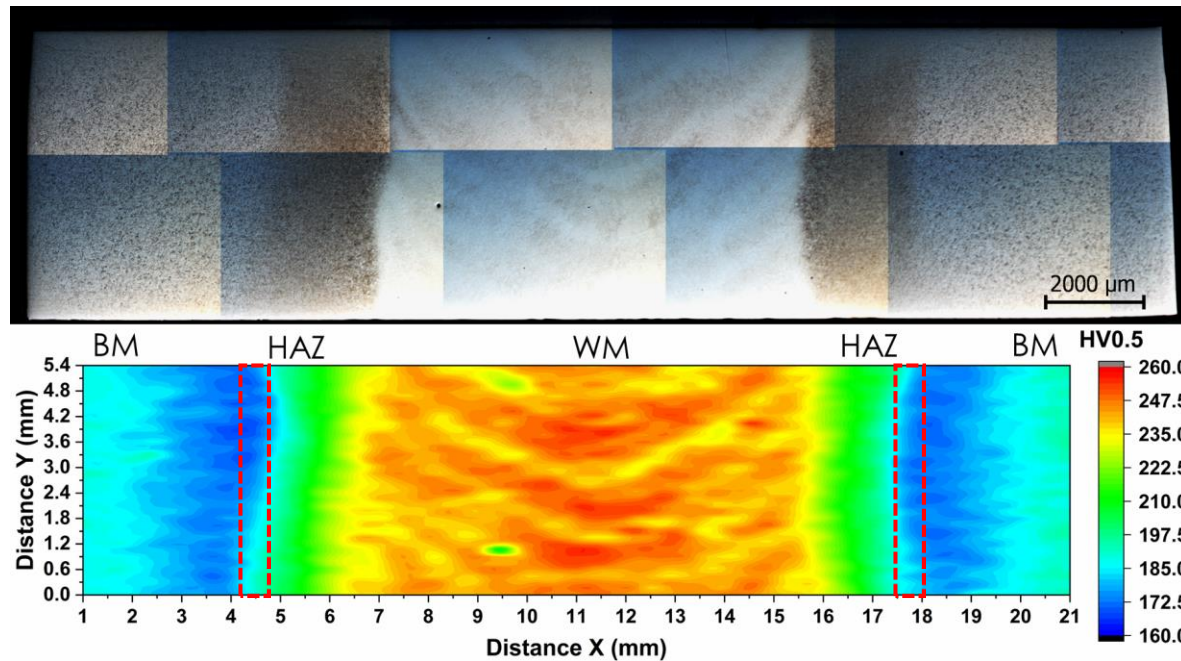
After creep testing

Creep strain localization in the HAZ quantified by high temperature DIC

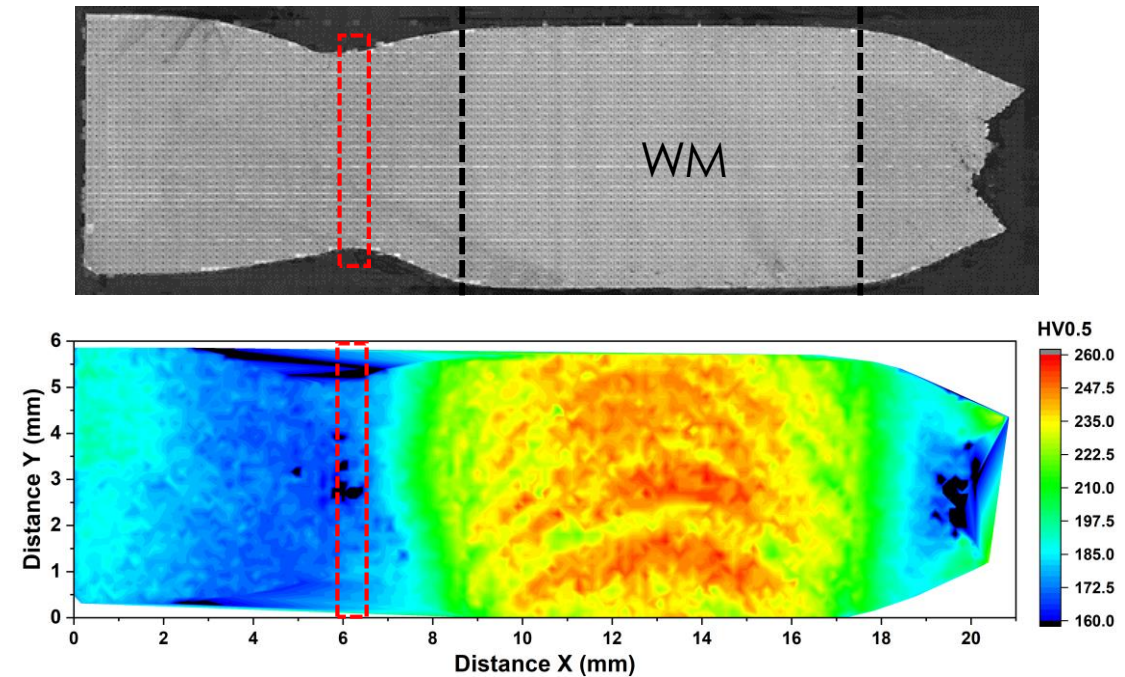


Local creep curves in different regions of weld, HAZ and base metal with a spatial resolution below 1mm

Systematic microhardness measurement helps to identify creep rupture location in the welds

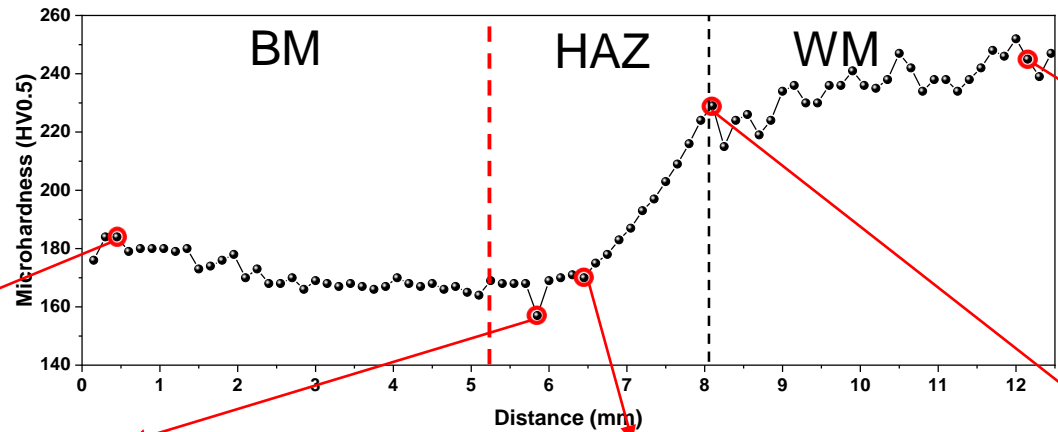


Before creep testing
PWHT-ed: 760 °C-2 h

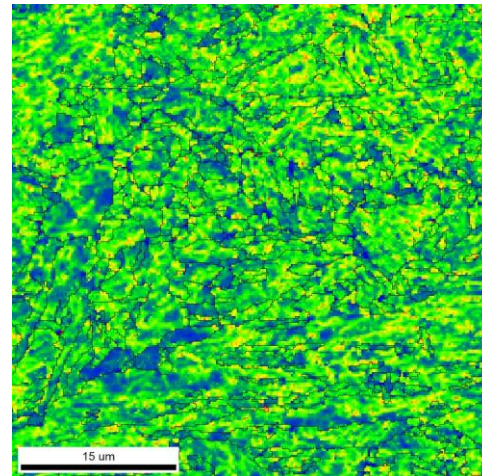
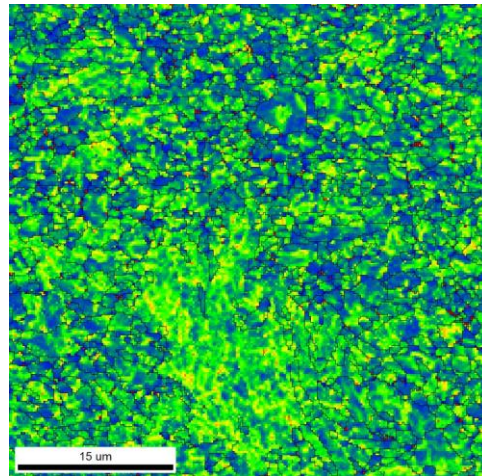
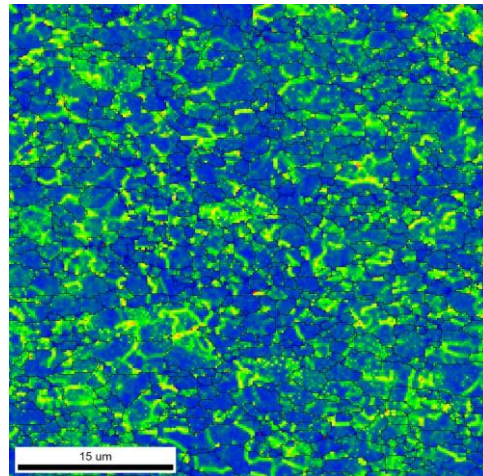
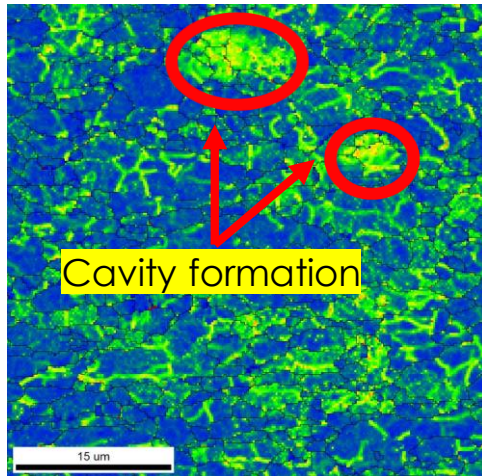
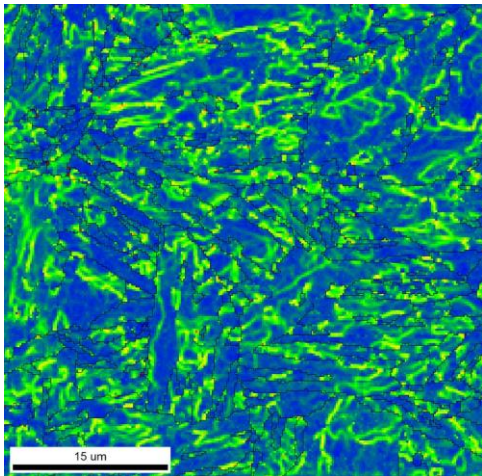
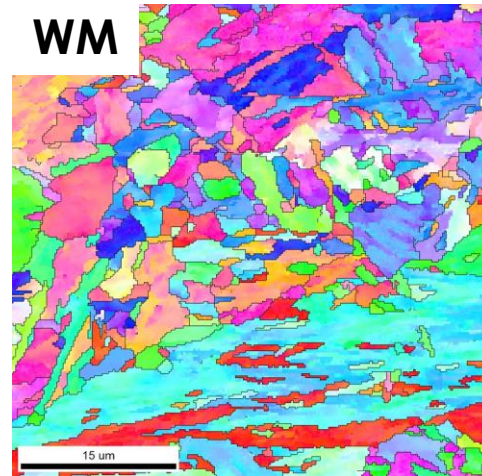
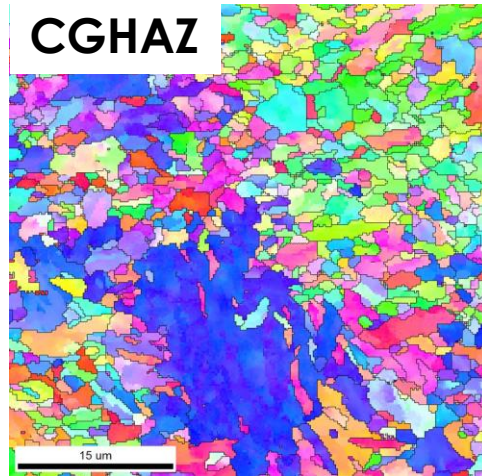
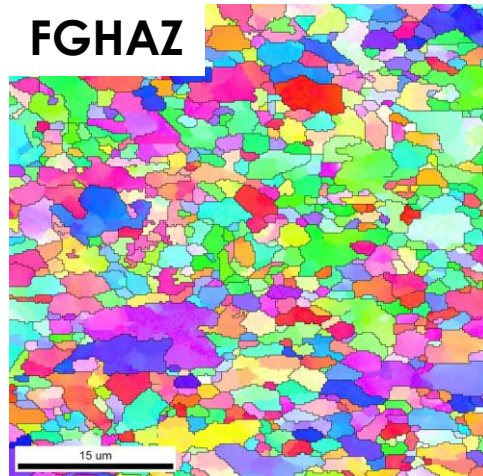
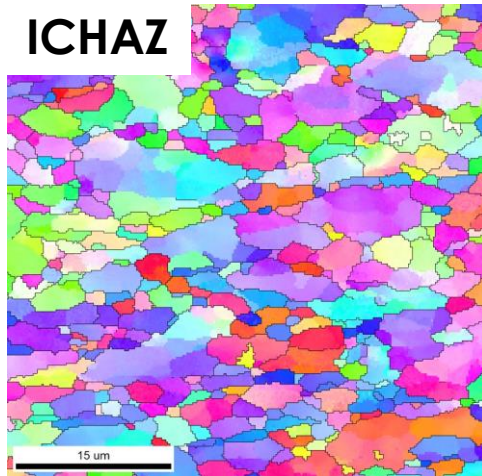
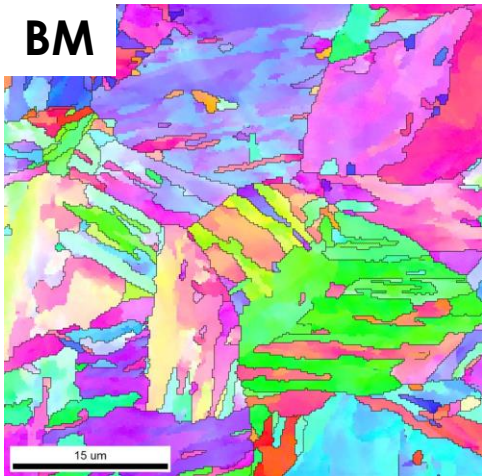


After creep testing
Creep: 600 °C-135 MPa

Hardness Distribution

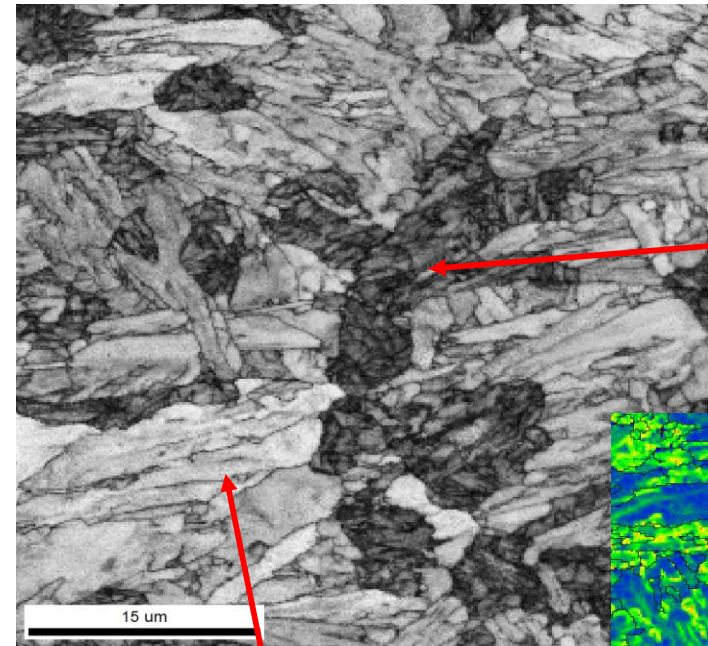
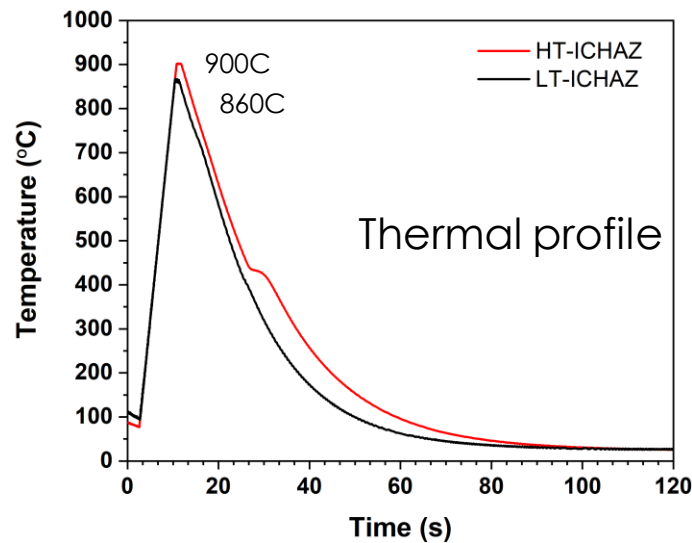
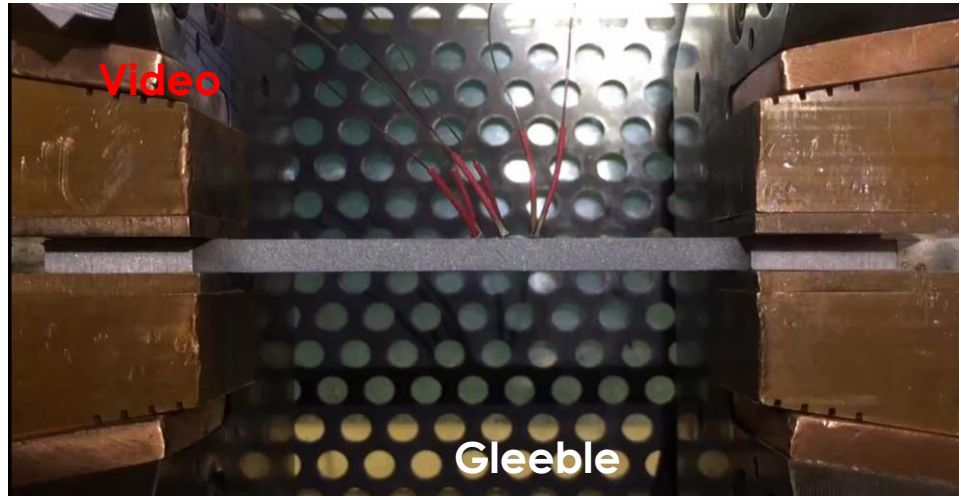


Structural Evolution



Purposely designed experiments with varying microstructures to support and validate the ICWE model

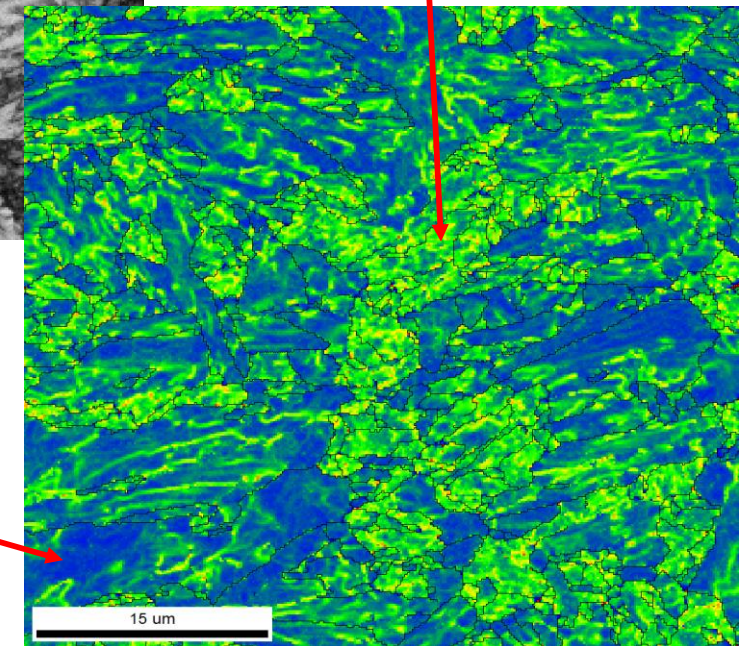
- Gleeble simulation of HAZ



LT Intercritical Thermal Cycle

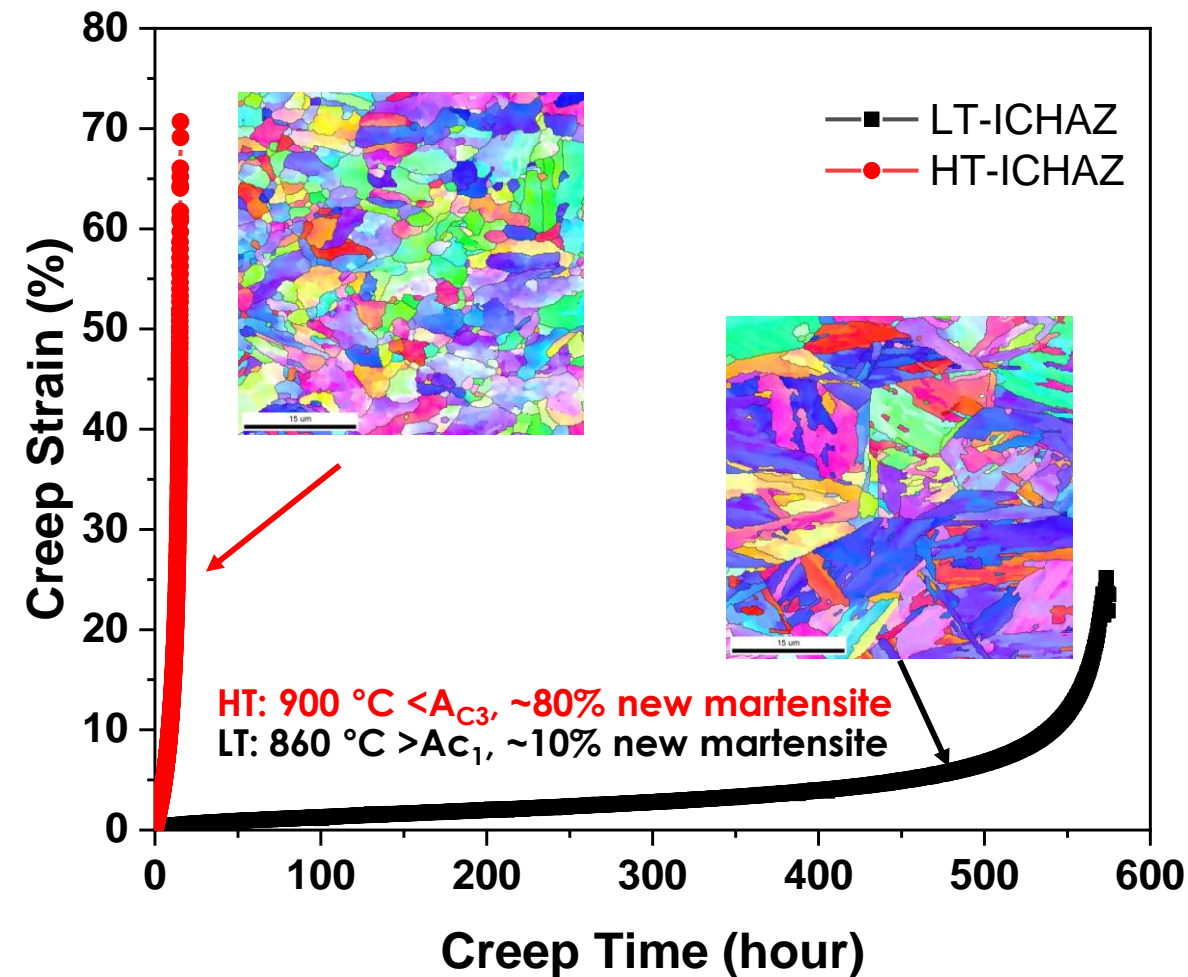
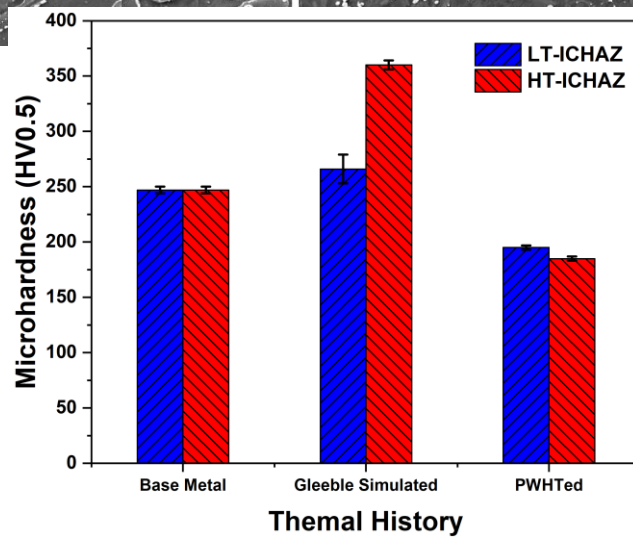
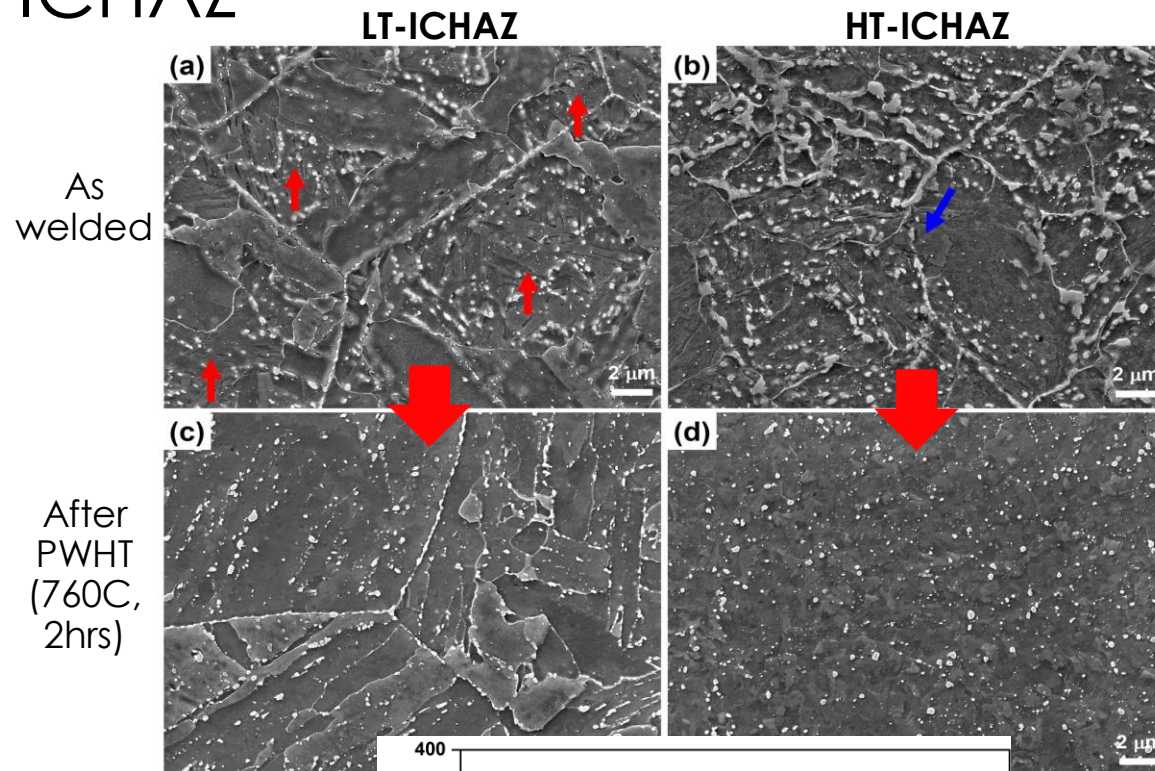
“New” martensite

“Old” tempered martensite



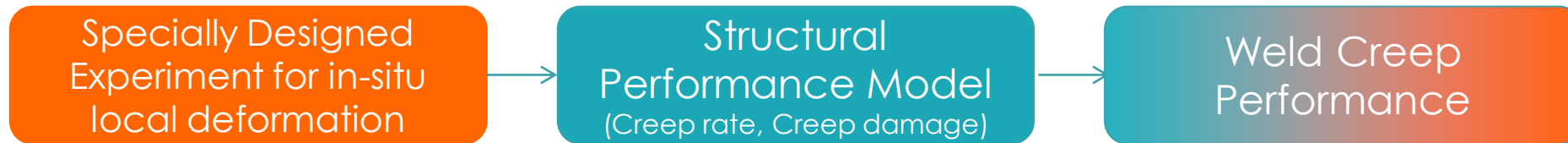
HT: 900 °C < A_{C3} , ~80% new martensite
LT: 860 °C > A_{C1} , ~10% new martensite

Different creep behavior related to formation of martensite in ICHAZ

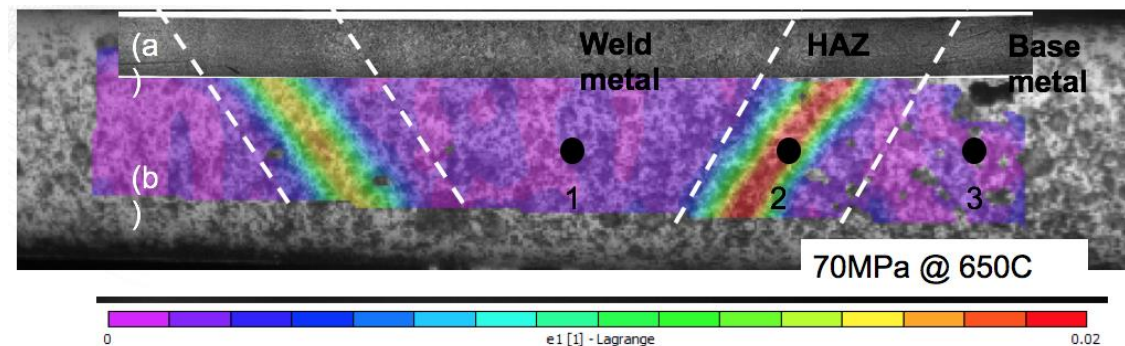


Additional creep tests for different HAZ microstructure constituents are on-going to extract information for model development and validation

Level 1 Model: An engineering (phenomenological) approach based on local weld creep measurement



- Experimentally determine the local creep strain evolution at different stages of creep deformation and failure
 - High temperature DIC based fully field, in-situ measurement across the entire weld/HAZ region
- Measured properties can be incorporated in constitutive equations or used as direct input in finite element models.



Level 1 Model: Creep Damage Model based on local weld creep measurement

- Physics based phenomenological constitutive equation

$$\dot{\varepsilon}_{ij} = A \sinh\left(\frac{B\sigma_e(1-H)}{(1-\phi)(1-\omega)}\right) \frac{3S_{ij}}{2\sigma_e}$$

$$\frac{dH}{dt} = \frac{h\dot{\varepsilon}_e}{\sigma_e} \left(1 - \frac{H}{H^*}\right) \quad \text{- Strain hardening}$$

$$\frac{d\phi}{dt} = \frac{K_c}{3} (1-\phi)^4 \quad \text{- Precipitate coarsening}$$

$$\frac{d\omega}{dt} = CN\dot{\varepsilon}_e(\sigma_I/\sigma_e)^\nu \quad \text{- Intergranular cavitation}$$

- Determination of material parameters

Optimization objective function

Genetic algorithm - Matlab

$$f(\varepsilon) = \sum_{i=1}^{n_i} \sum_{j=1}^{m_j} \left[(\varepsilon_{ij}^f - \varepsilon_{ij}^e) / \varepsilon_{ij}^e \right]^2$$

ε_{ij}^e - Experiment creep strain

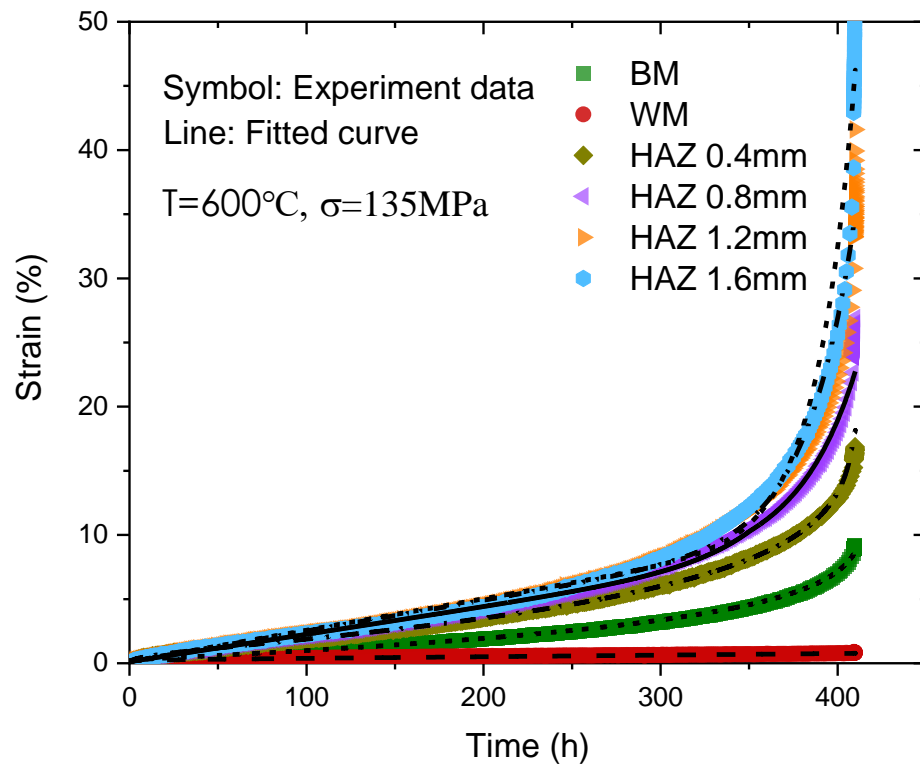
ε_{ij}^f - Fitted value of creep strain

n_i - Number of experiment curves

m_j - Number of data points on experiment curves

Determination of material parameters from local DIC creep measurement

- Comparison



(Distance from the fusion line)

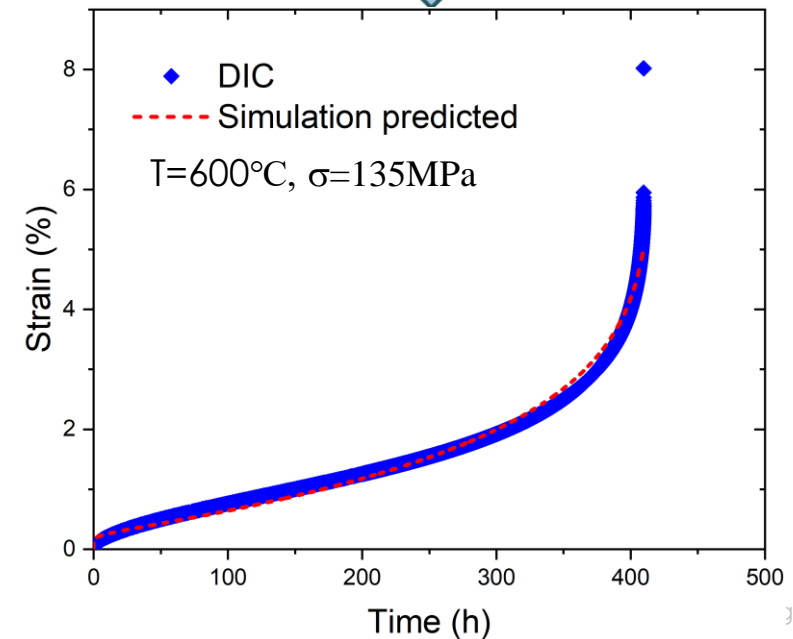
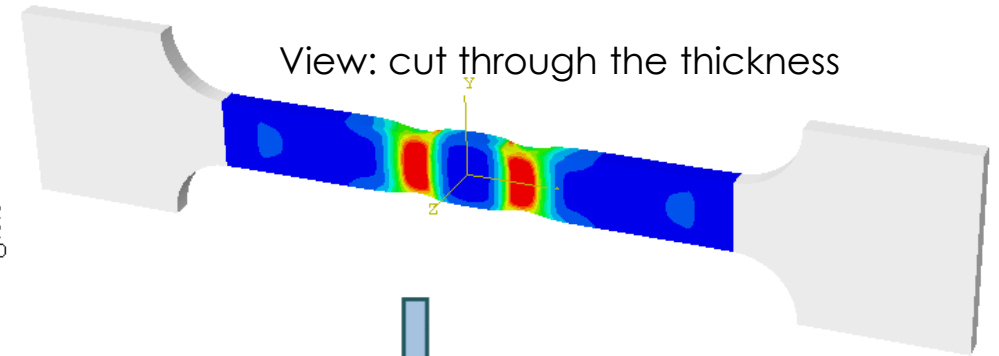
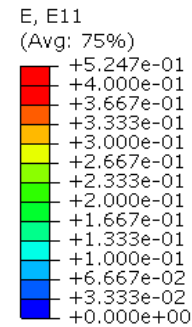
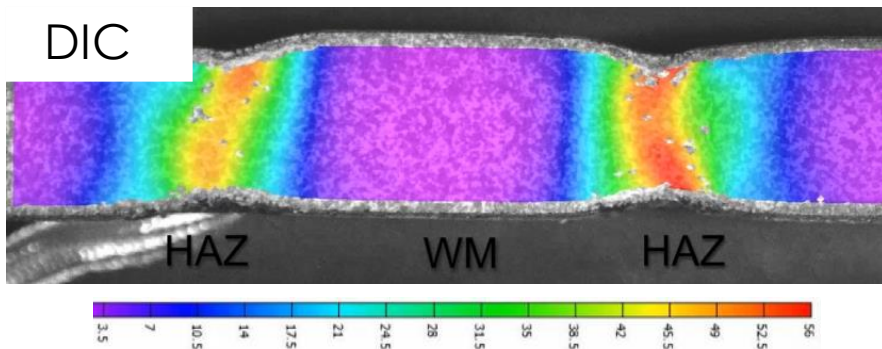
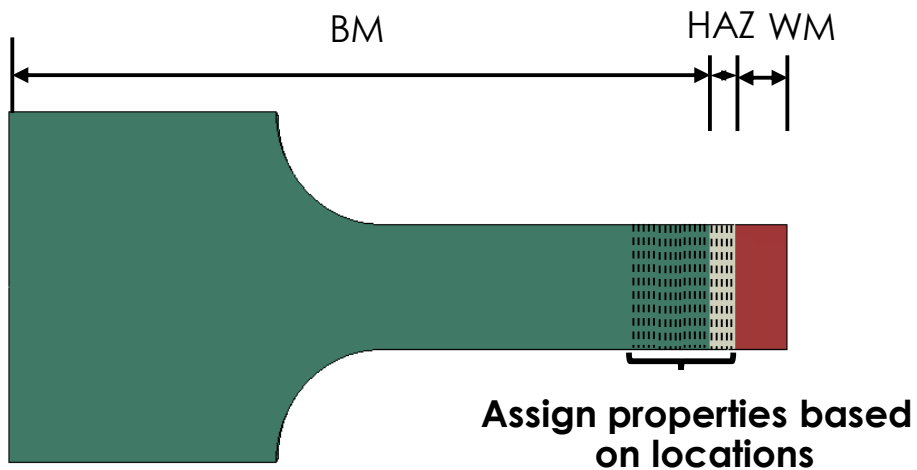
- Constitutive parameters

	A (h ⁻¹)	B (MPa ⁻¹)	C	h (MPa)	H*	K _c (h ⁻¹)
WM	2.9563×10 ⁻⁹	1.1520×10 ⁻¹	1.1804	9.3605×10 ⁴	0.4266	2.9786×10 ⁻⁶
BM	1.4059×10 ⁻⁸	1.1735×10 ⁻¹	1.3411	9.0098×10 ⁴	0.4275	8.9785×10 ⁻⁶
HAZ (0.4mm)	3.8059×10 ⁻⁸	1.3935×10 ⁻¹	2.0416	2.010×10 ⁴	0.5473	8.9785×10 ⁻⁶
HAZ (0.8mm)	3.9287×10 ⁻⁸	1.3935×10 ⁻¹	2.0535	2.010×10 ⁴	0.5476	1.0978×10 ⁻⁵
HAZ (1.2mm)	4.2859×10 ⁻⁸	1.3935×10 ⁻¹	2.0240	1.6098×10 ⁴	0.5507	1.2982×10 ⁻⁵
HAZ(1.6-2.0mm)	4.2859×10 ⁻⁸	1.3935×10 ⁻¹	2.0262	1.6098×10 ⁴	0.5514	1.3980×10 ⁻⁵

$$(0 < H < H^*, 0 < \phi < 1, 0 < \omega < 1/3, \nu = 2.8)$$

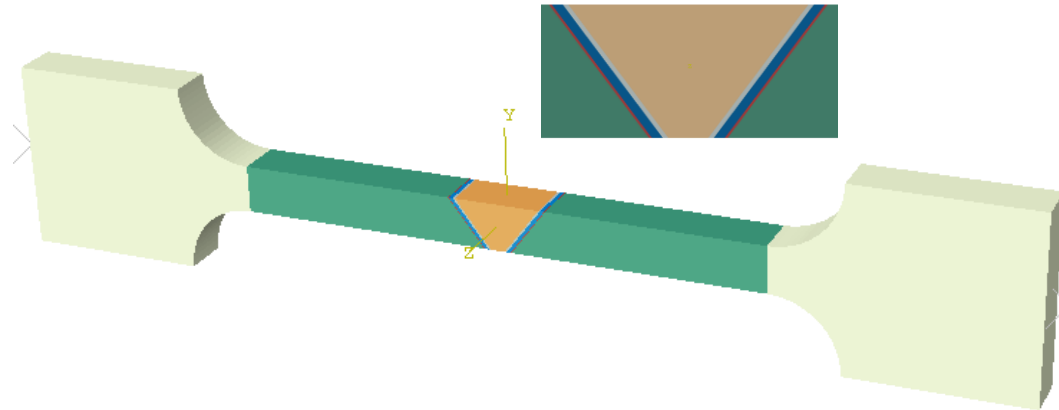
Comparison: Level I Model and DIC Experiment

- Finite element model

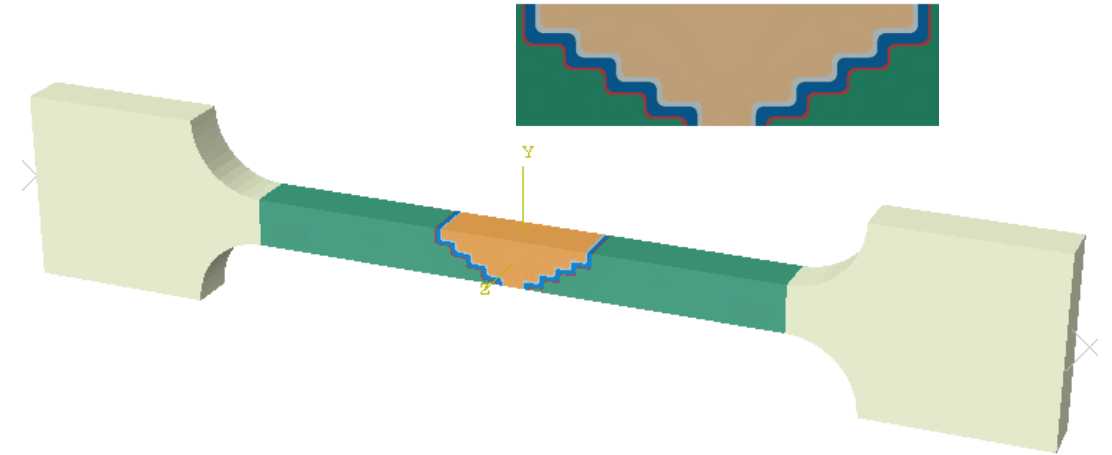


Application of Level 1 Model: An improved weld configuration?

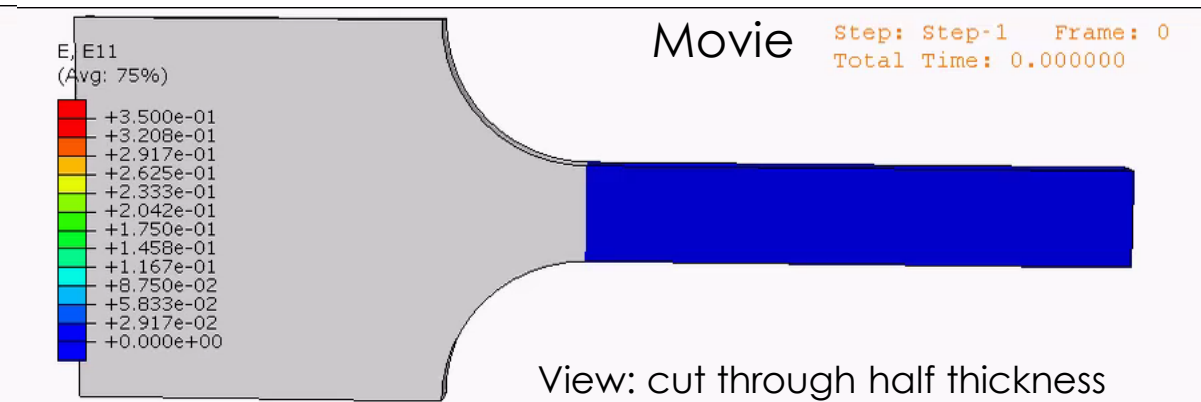
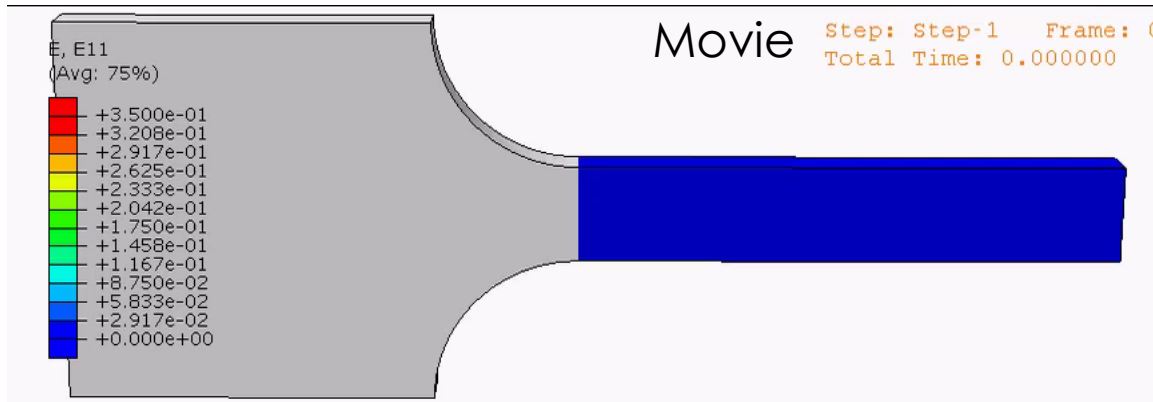
- Groove weld



- Step weld

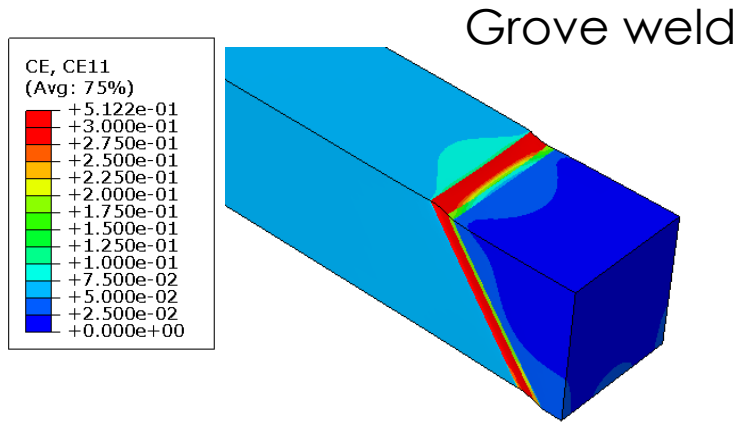


Simulation results

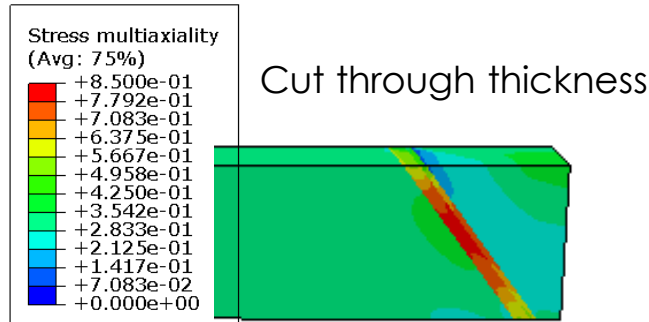


An improved weld configuration?

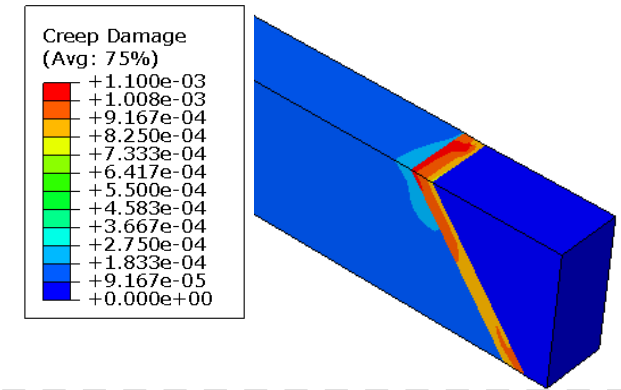
- Creep strain



- Stress triaxiality

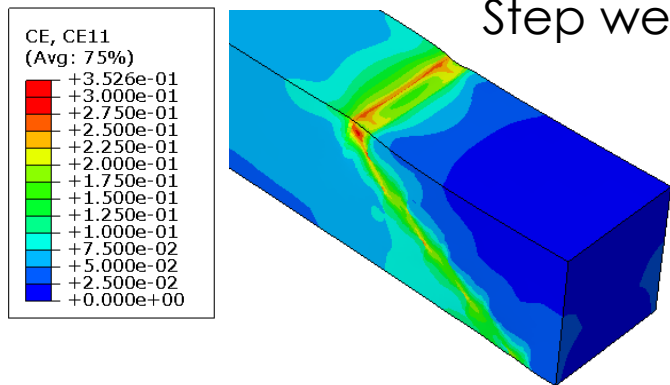


- Creep damage parameter ω



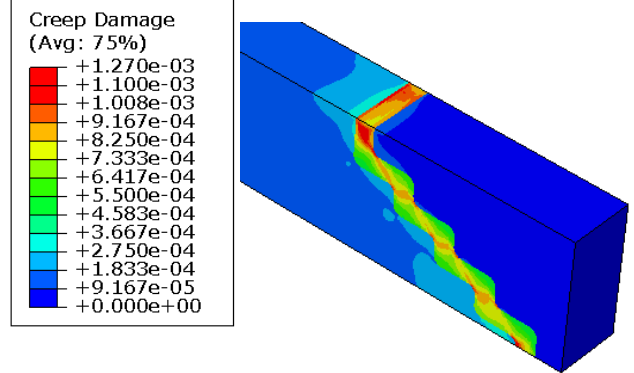
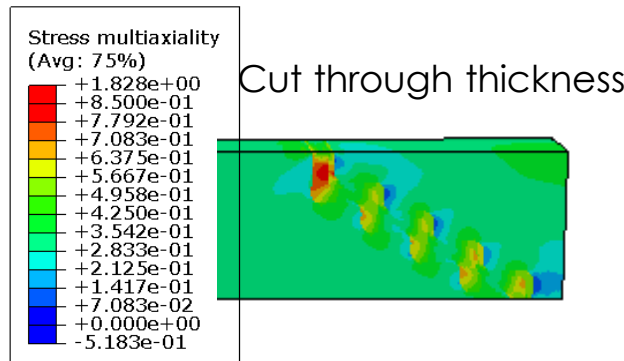
- Creep strain

Step weld

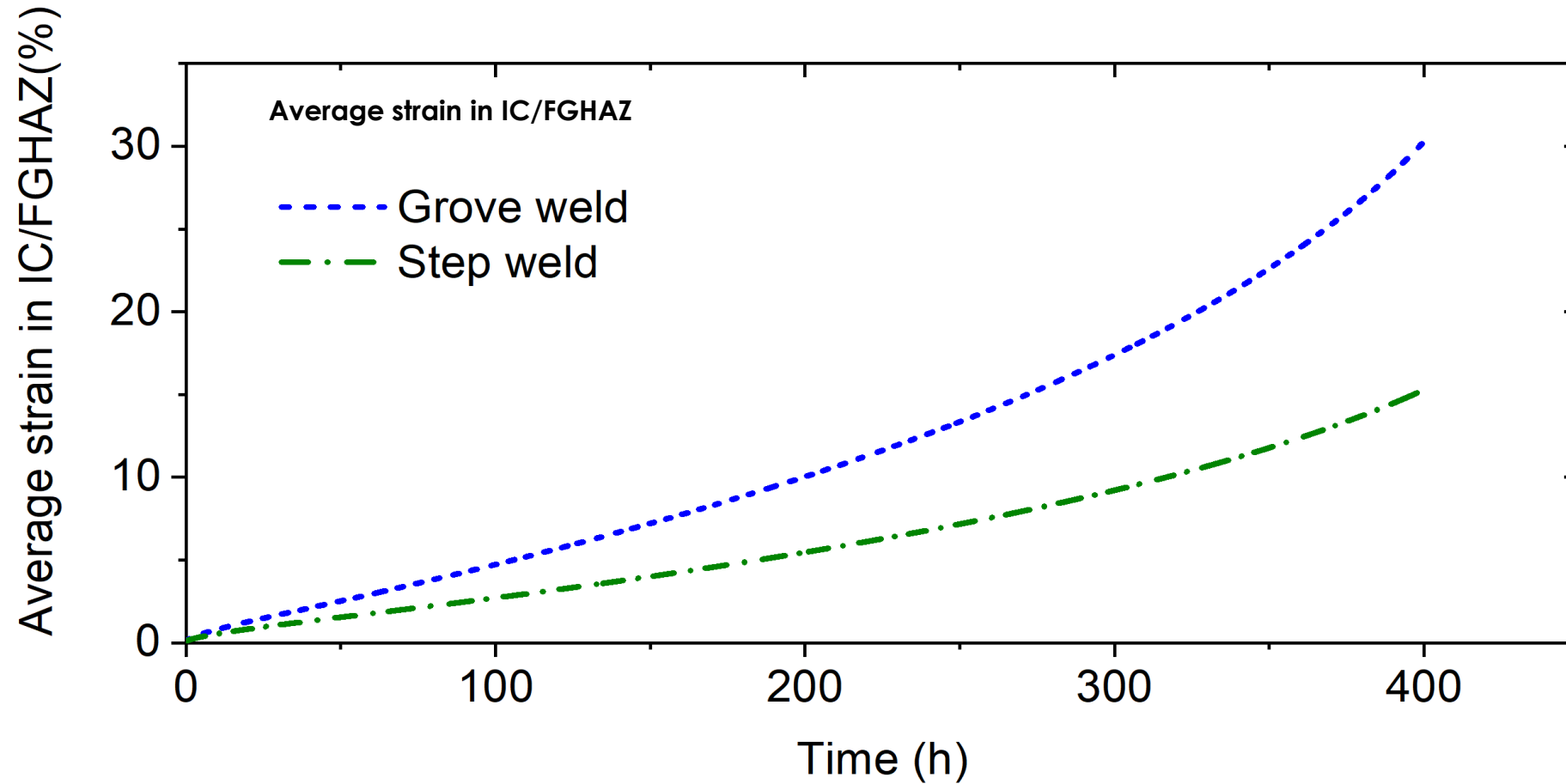


- Stress triaxiality

Cut through thickness



An Improved weld configuration?

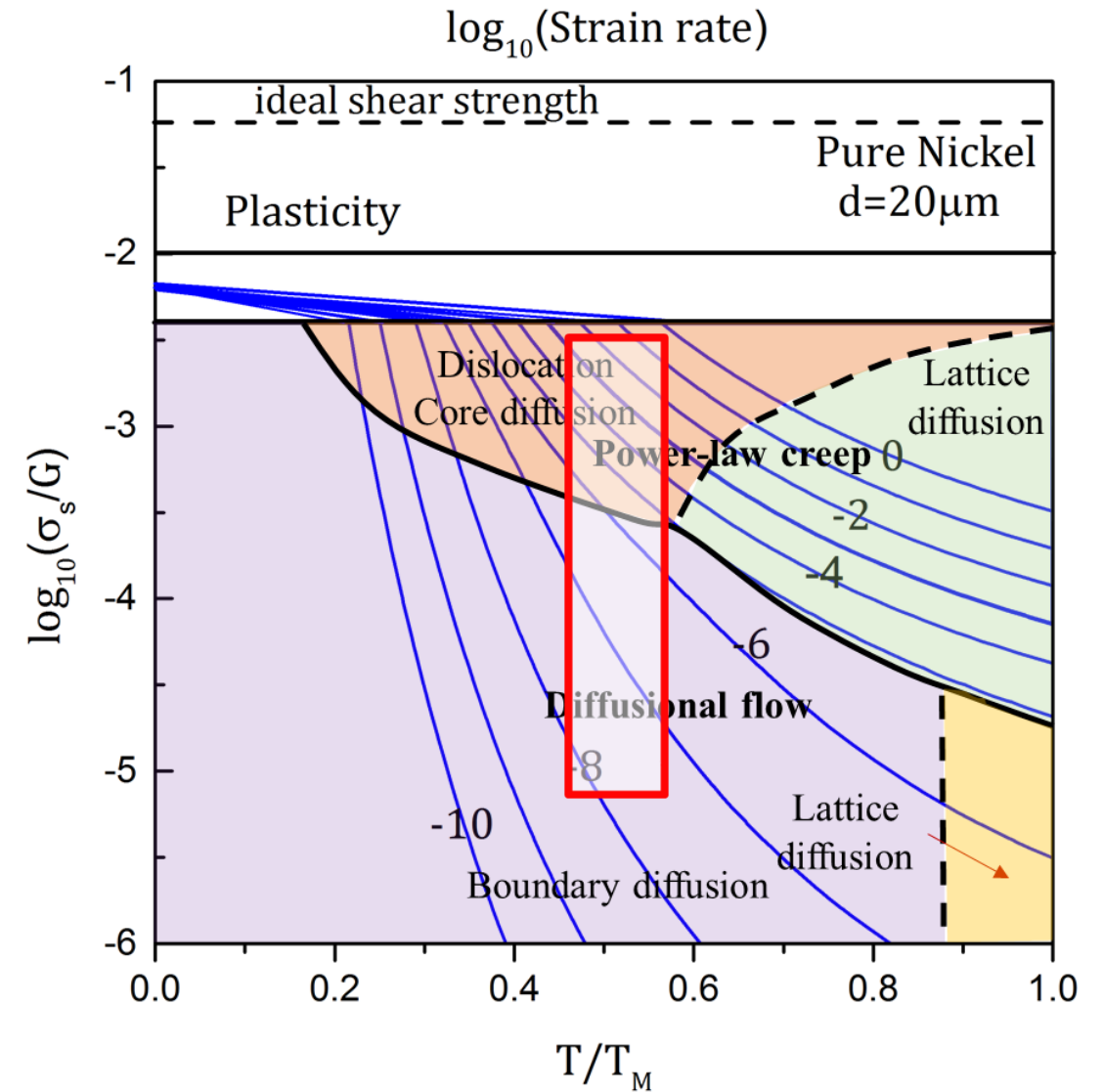
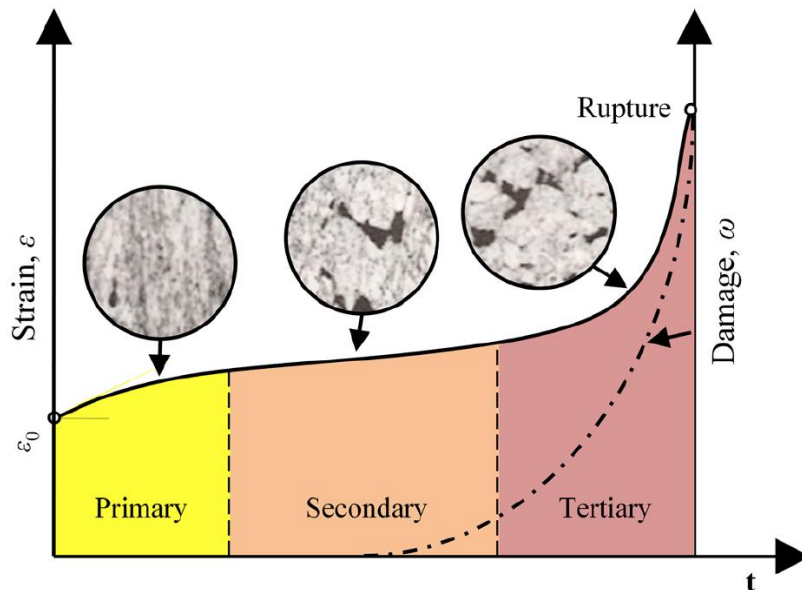


Level 2 Model: Life Prediction with Explicit Microstructure Information

- What are the key microstructure features for creep deformation?
- How does these key features affect creep properties?
- Due to significant microstructure variations in the weld region, it is essential to explicitly incorporate the microstructure information in creep life prediction
- Such model is also useful to design and optimize microstructure for creep life improvement (base metal and weld metal)

Level 2 Macroscopic Creep Deformation and Damage Model

- Two Major Parts
 - Creep deformation
 - Grain interior
 - Grain boundary
 - Cavitation failure
 - Cavity nucleation
 - Cavity growth
 - Grain boundary failure



Deformation and Fracture Mechanism Map

Part I: Creep Model - Deformation Mechanisms

- Governing constitutive equation:

Grain interior creep

$$\sigma_{ij,i} + b_j = 0,$$

$$\varepsilon_{ij} = \frac{1}{2}(u_{i,j} + u_{j,i}),$$

$$\dot{\varepsilon}_{ij} = \dot{\varepsilon}_{ij}^e + \dot{\varepsilon}_{ij}^p,$$

$$\dot{\varepsilon}_{ij}^e = \frac{1+\nu}{E} \left(\dot{\sigma}_{ij} - \frac{\nu}{1+\nu} \dot{\sigma}_{kk} \delta_{ij} \right).$$

$$\dot{\varepsilon}_{ij}^p = \left[A_{\text{dis}} \frac{EbD_1}{k_B T} \left(\frac{\sigma_e}{E} \right)^n + A_{\text{coble}} \frac{EbD_{\text{gb}}}{k_B T} \left(\frac{b}{d} \right)^3 \left(\frac{\sigma_e}{E} \right) \right] \frac{3S_{ij}}{2\sigma_e}$$

where $S_{ij} = \sigma_{ij} - \sigma_{kk} \delta_{ij} / 3$, $\sigma_e = \sqrt{3S_{ij}S_{ij}/2}$.

Grain boundary sliding

Newtonian viscous flow

$$\dot{u}_s = \frac{\Omega \eta_0 \exp(-Q_{\text{gb}}/RT)}{k_B T} \tau$$

- Grain orientation effects:

$$f_{\text{taylor}} = \frac{\sum \gamma^{\text{local}}}{\langle \varepsilon_{\text{VM}}^{\text{local}} \rangle} \quad \text{-- Indicates "soft" or "hard" grains.}$$

- Crystal plasticity theory
- Multiplicative decomposition:

$$\mathbf{F} = \mathbf{F}^e \mathbf{F}^p$$

- Plastic deformation rate:

$$\dot{\mathbf{F}}^p \mathbf{F}^{p-1} = \sum_{\alpha} \dot{\gamma}^{(\alpha)} \mathbf{s}^{(\alpha)} \otimes \mathbf{m}^{(\alpha)}$$

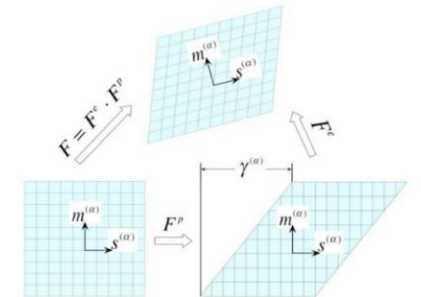
- Flow rule
- Hardening law

$$\dot{\gamma}^{\alpha} = \dot{\gamma}_0 \left(\frac{\tau^{\alpha}}{g^{\alpha}} \right)^{1/m} \quad \dot{g}^{\alpha} = \sum_{\beta} h_{\alpha\beta} |\dot{\gamma}^{\beta}|$$

- Modification to the rate equation

$$\dot{\varepsilon}_{ij}^p = \left[A_{\text{dis}} \bar{f}_{\text{local}}^1 \frac{EbD_1}{k_B T} \left(\frac{\sigma_e}{\sigma_0} \right)^n + A_{\text{coble}} \frac{EbD_{\text{gb}}}{k_B T} \left(\frac{b}{d} \right)^3 \left(\frac{\sigma_e}{E} \right) \right] \frac{3S_{ij}}{2\sigma_e}$$

where $\bar{f}_{\text{local}}^1 = f_{\text{local}}^1 / \max(f_{\text{local}}^1, f_{\text{local}}^2, \dots, f_{\text{local}}^1, \dots, f_{\text{local}}^N)$



Part II: Creep Fracture and Life Prediction by the Intergranular Creep Fracture Model

Grain interior creep

$$\dot{\epsilon}_{ij} = \dot{\epsilon}_{ij}^e + \dot{\epsilon}_{ij}^p$$

$$\dot{\epsilon}_{ij}^e = \frac{1+\nu}{E} \left(\dot{\sigma}_{ij} - \frac{\nu}{1+\nu} \dot{\sigma}_{kk} \delta_{ij} \right)$$

$$\dot{\epsilon}_{ij}^p = \dot{\epsilon}_0 \left(\frac{\sigma_e}{\sigma_0} \right)^n \frac{3}{2} \frac{S_{ij}}{\sigma_e} M$$

where $\sigma_e = \sqrt{\frac{3}{2} S_{ij} S_{ij}}$

**M: Micromechanical Taylor factor
- Grain orientation**

Grain boundary sliding

Newtonian viscous flow

$$\dot{u}_s = w \frac{\tau}{\eta}, \quad \frac{1}{\eta} = \frac{A}{T} e^{-\frac{Q_s}{RT}}$$

Cavity representation

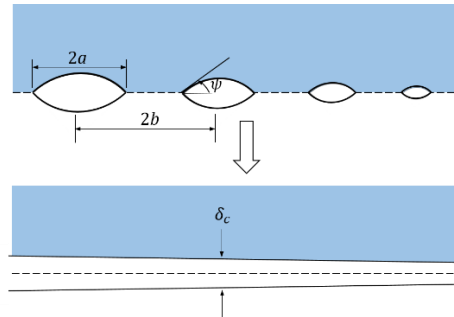
Cavity volume $V = \frac{4}{3} \pi a^3 h(\psi)$

Shape parameter $h(\psi) = \frac{\left[(1 + \cos \psi)^{-1} - \frac{1}{2} \cos \psi \right]}{\sin \psi}$

Smear-out separation $\dot{u}_n = \frac{\dot{V}}{\pi b^2} - \frac{2V\dot{b}}{\pi b^3}$

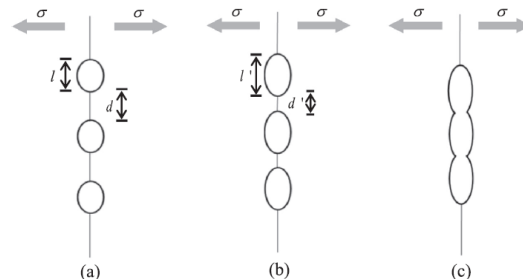
Rate of void spacing

$$\frac{\dot{b}}{b} = \frac{1}{2} (\dot{\epsilon}_I + \dot{\epsilon}_{II}) - \frac{1}{2} \frac{\dot{N}}{N}$$



Damage evolution:

$a/b \sim 1.0$



Cavity nucleation, growth and coalescence

Cavity nucleation

Cavitation nucleation rate: $\dot{N} = F_n \left(\frac{\sigma_n}{\sum_0} \right)^2 \dot{\epsilon}_e^c$

Nucleation parameter: $S = \left(\frac{\sigma_n}{\sum_0} \right)^2 \dot{\epsilon}_e^c$ for $\sigma_n > 0$

Threshold value: $S_{thr} = \frac{N_i}{F_n}$

Cavity nucleation to be triggered: $S > S_{thr}, N < N_{max}$

Cavity growth

Cavity growth – GB diffusion and creep:

$$\dot{V} = \dot{V}_1 + \dot{V}_2$$

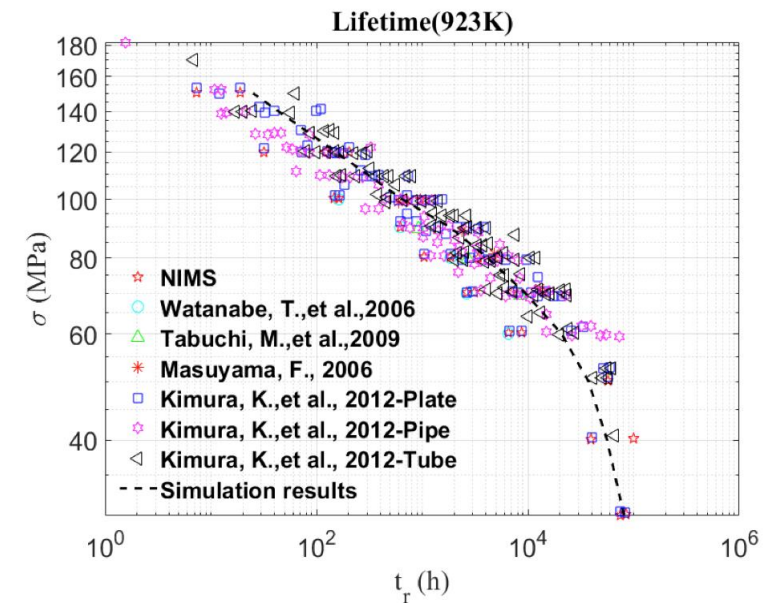
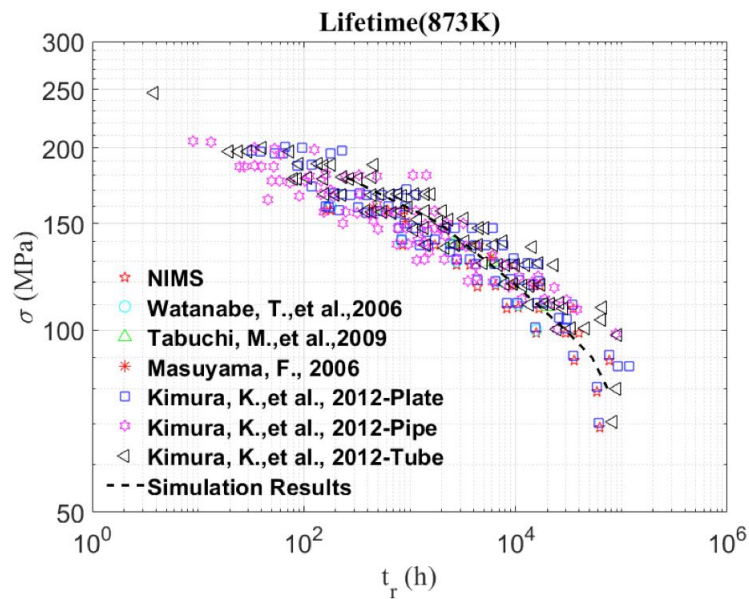
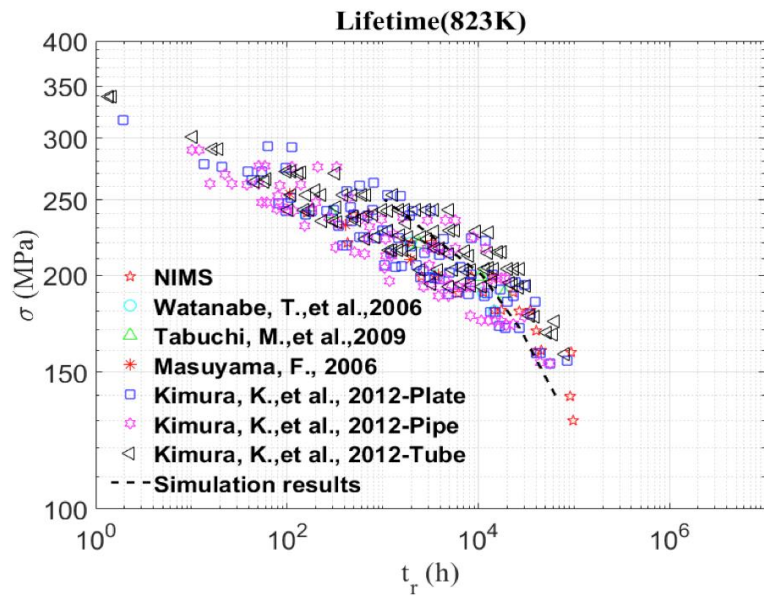
1. Contribution of GB diffusion:

$$\dot{V}_1 = 4\pi D \frac{\sigma_n - (1-f)\sigma_s}{\ln\left(\frac{1}{f}\right) - \frac{1}{2}(3-f)(1-f)}$$

2. Contribution of creep deformation:

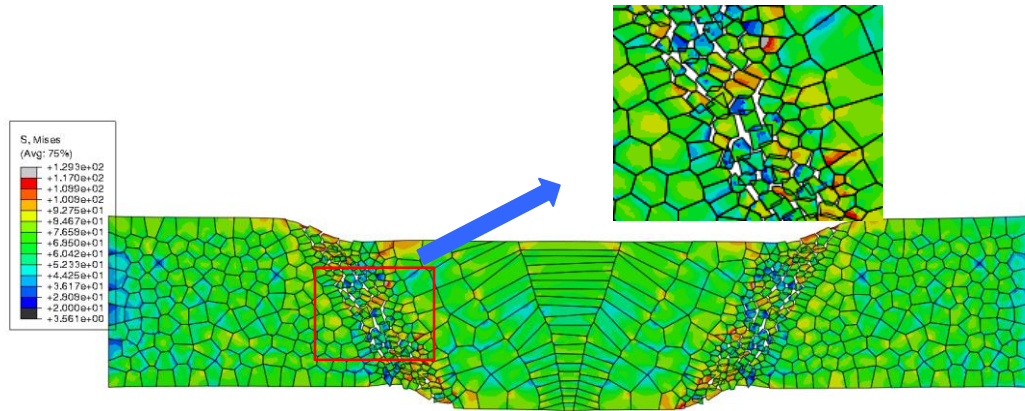
$$\dot{V}_2 = \begin{cases} \pm 2\pi \dot{\epsilon}_e^c a^3 h(\psi) \left[\alpha_n \left| \frac{\sigma_m}{\sigma_e} \right| + \beta_n \right]^n, & \text{for } \pm \frac{\sigma_m}{\sigma_e} > 1 \\ 2\pi \dot{\epsilon}_e^c a^3 h(\psi) [\alpha_n + \beta_n]^n \frac{\sigma_m}{\sigma_e}, & \text{for } \left| \frac{\sigma_m}{\sigma_e} \right| < 1 \end{cases}$$

Integrating pieces together for creep fracture (P91 base metal):

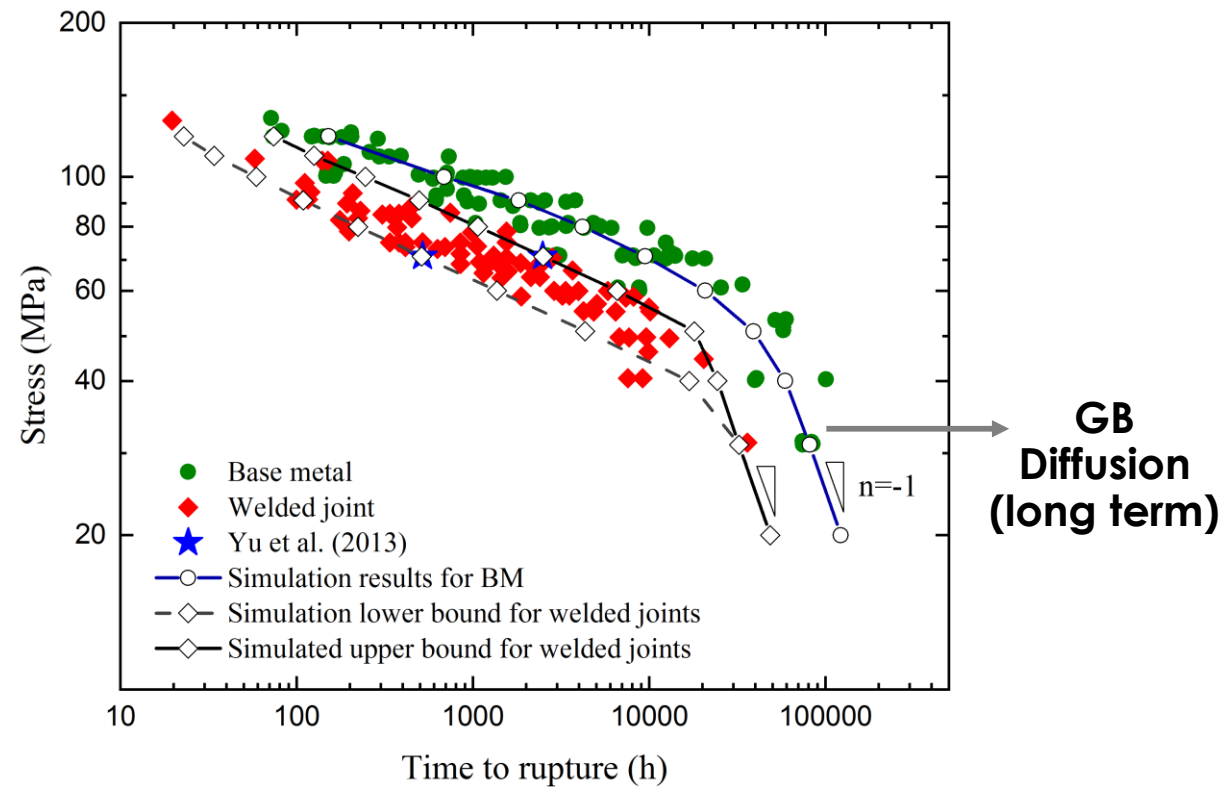
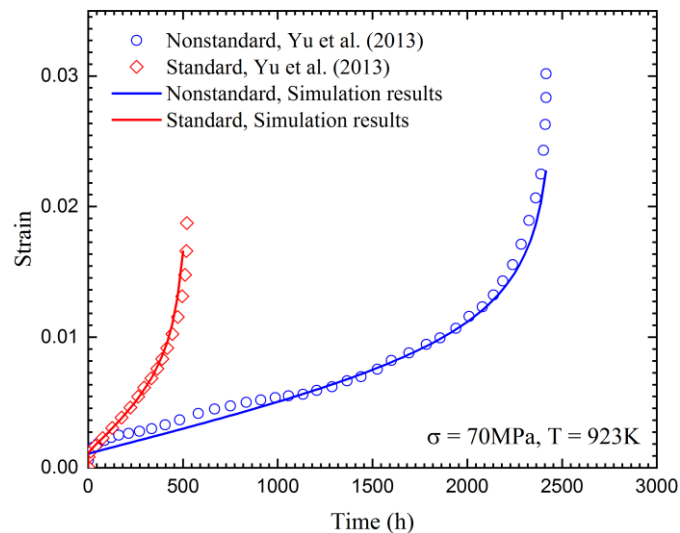


Creep Damage Simulation of Weld Type IV Failure

- Creep fracture in HAZ
- Life prediction

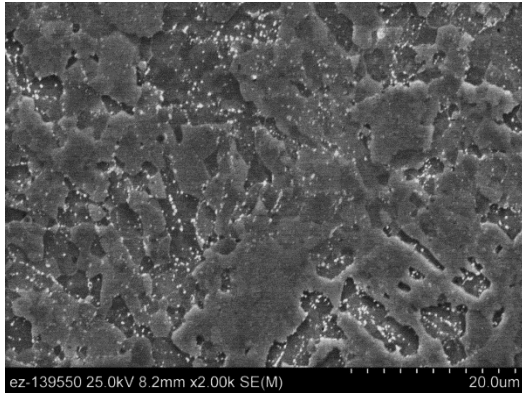


- Creep curve: predicted vs. experiment

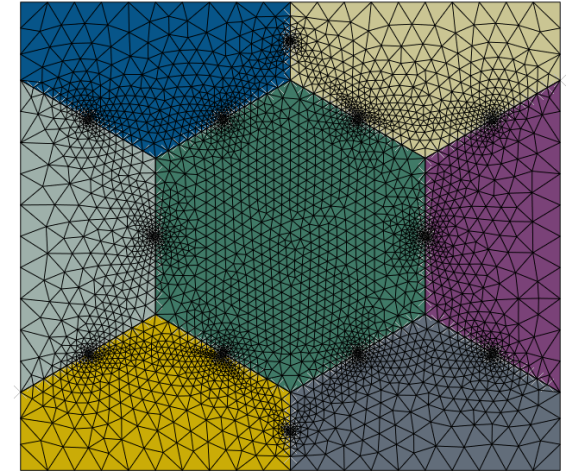


Level 2 Model Development

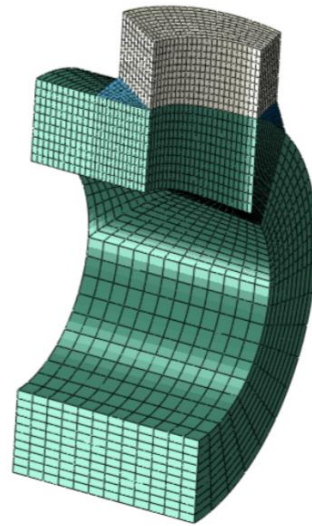
Microstructure Features



Representative Volume Element (RVE) explicitly connect with key microstructure features

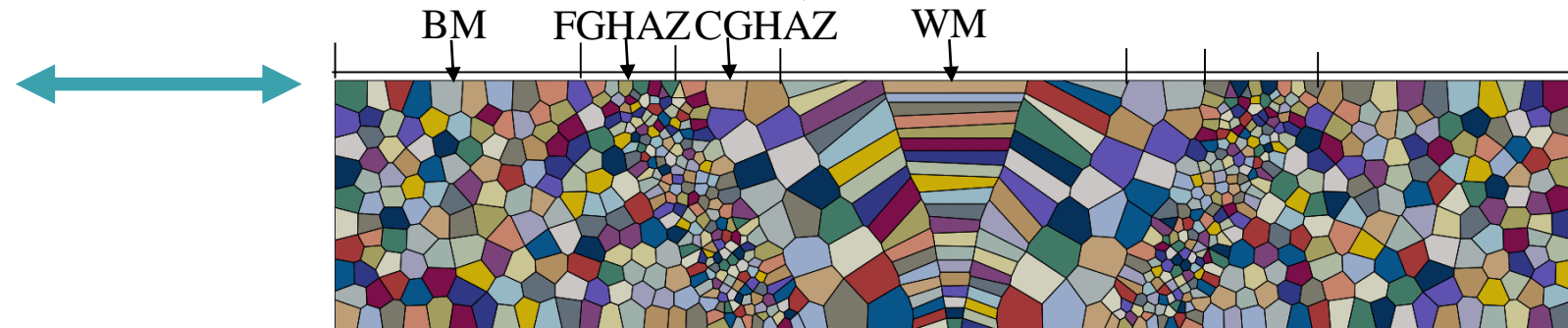


Constitutive creep relation from RVE
 $\dot{\epsilon}_{creep} = f(\text{carbides, grain boundary sliding, grain interior deformation, } T, \sigma, \text{ etc})$



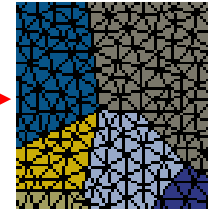
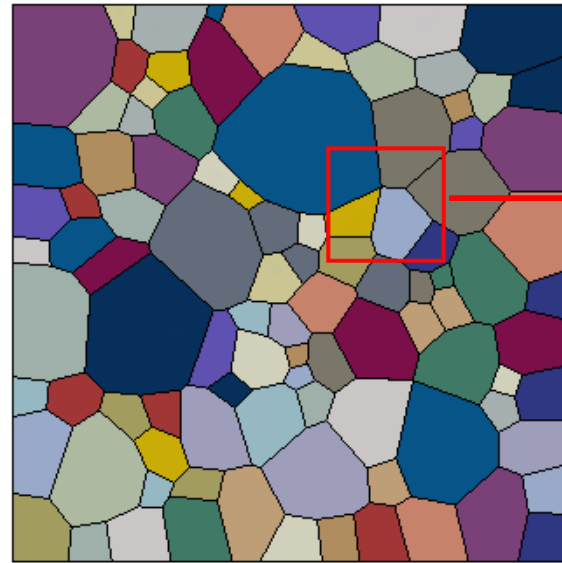
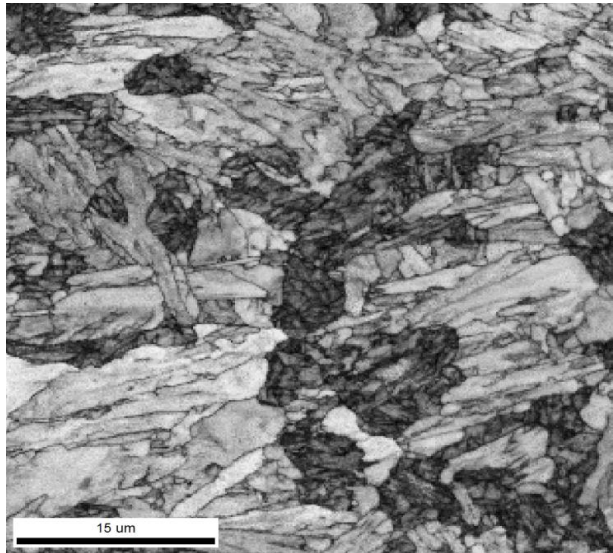
Structural Component

Weld Coupon



RVE Model to Study Creep Rupture Behavior in ICHAZ with Two Phases

- Level II RVE creep model with explicit microstructure Information



→ Phase A
→ Phase B
(35%A+65%B)

Case study:

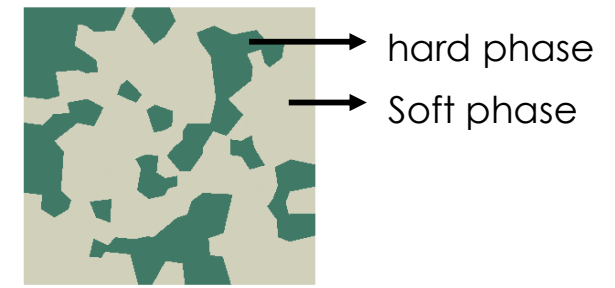
Case I: $\dot{\epsilon}_B = 10\dot{\epsilon}_A = 1.337 \times 10^{-8} s^{-1}$

Case III: $\dot{\epsilon}_A = \dot{\epsilon}_B = 1.337 \times 10^{-8} s^{-1}$

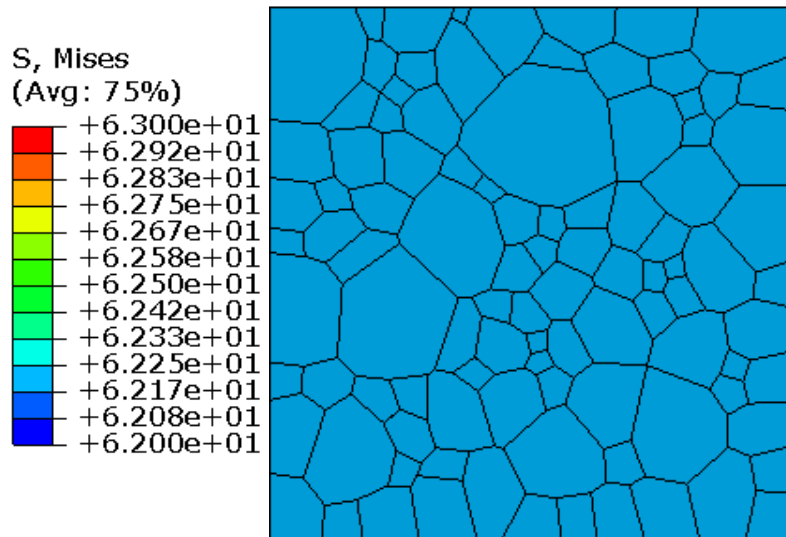
Phase A has lower creep rate (hard phase)

Phase A and B have same creep rate

Creep Rupture Behavior in ICHAZ: Case I, Time=1s

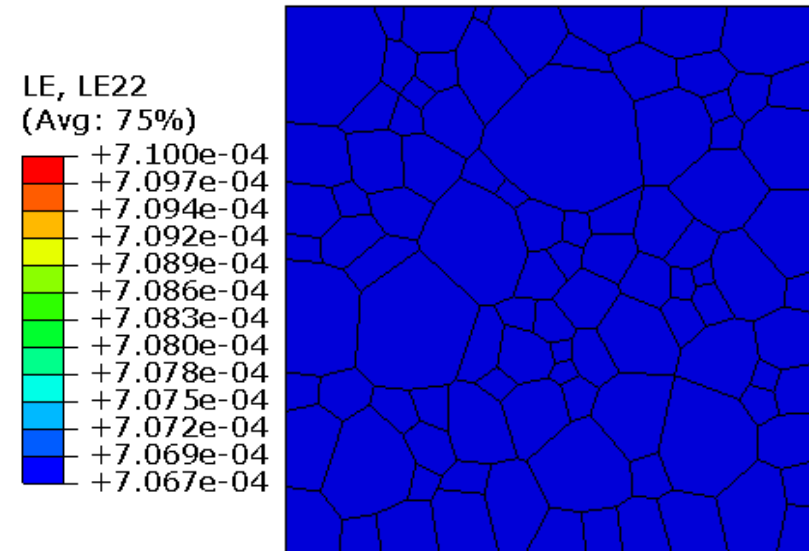


- Stress



- Strain

Case I: $\dot{\epsilon}_B = 10\dot{\epsilon}_A = 1.337 \times 10^{-8} s^{-1}$

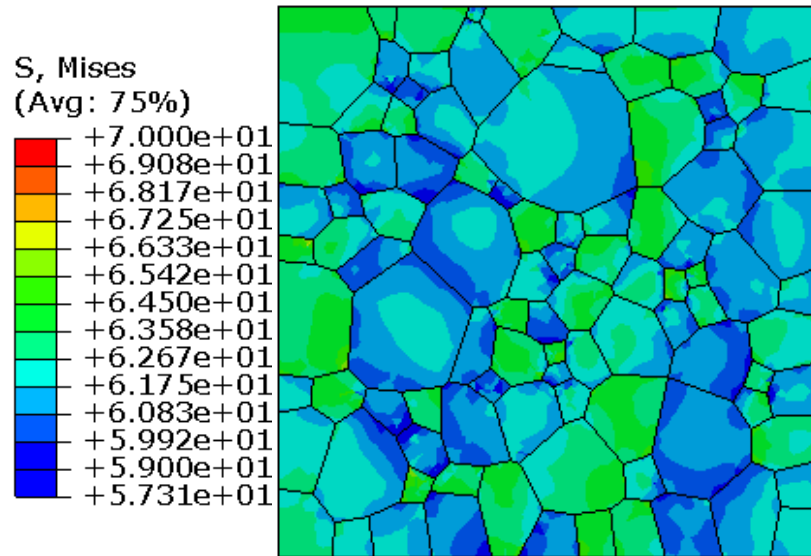


- Uniform stress and strain distribution at the beginning of loading due to the similar elastic material property.

Creep Rupture Behavior in ICHAZ: Case I, Time=4,433s

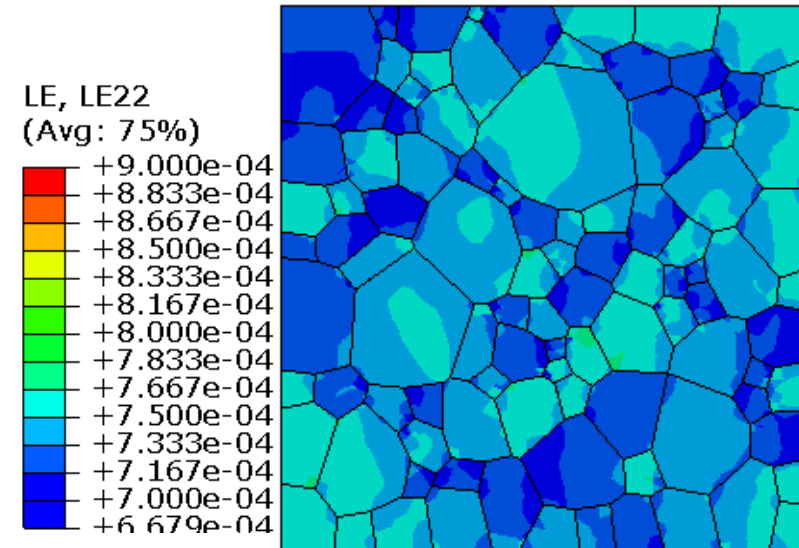


- Stress



- Strain

Case I: $\dot{\epsilon}_B = 10\dot{\epsilon}_A = 1.337 \times 10^{-8} s^{-1}$

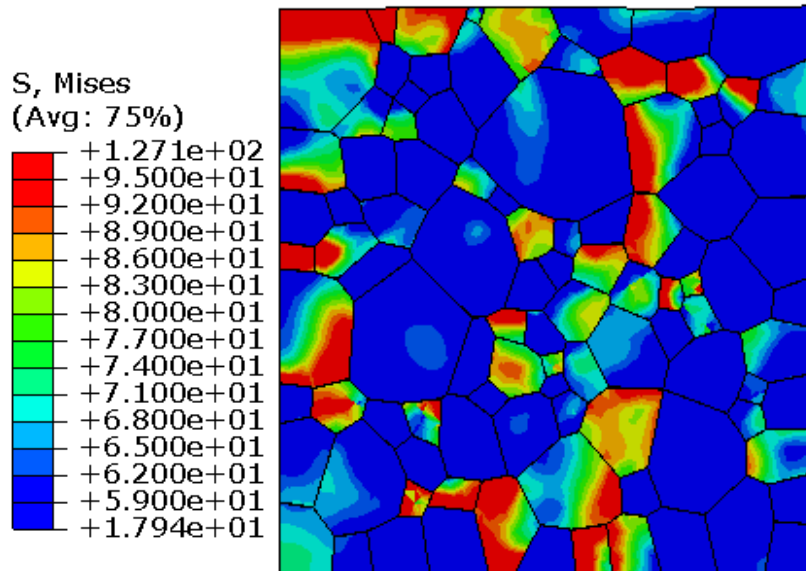


- Nonuniform stress distribution as a result of the creep rate difference between phase A and B. Higher stress is observed in the 'hard' phase, and higher strain is in the soft phase.

Creep Rupture Behavior in ICHAZ: Case I, Time=263,600 s

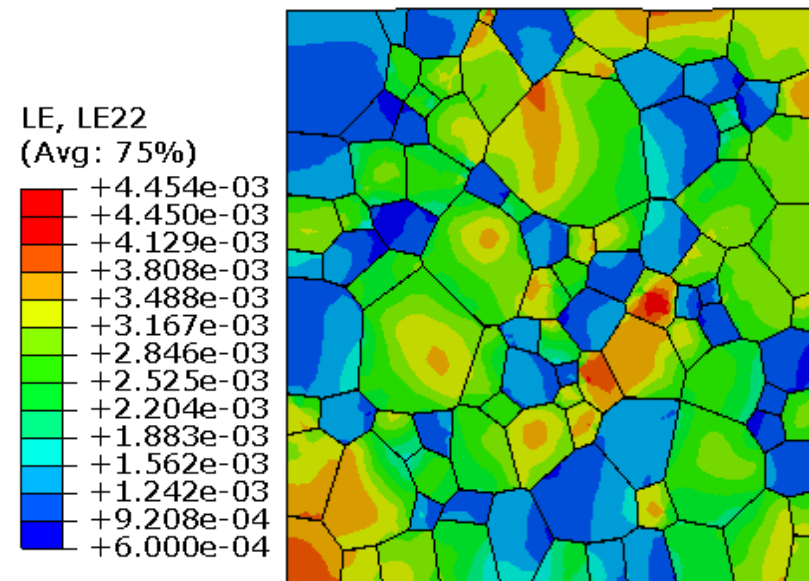


• Stress



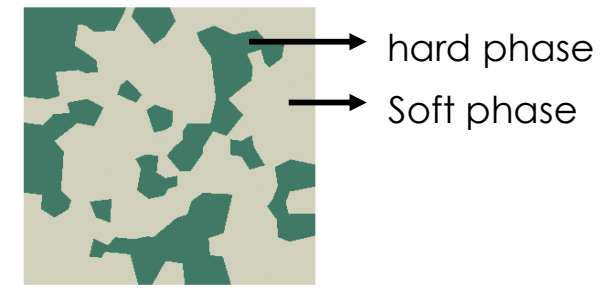
• Strain

Case I: $\dot{\epsilon}_B = 10\dot{\epsilon}_A = 1.337 \times 10^{-8} s^{-1}$

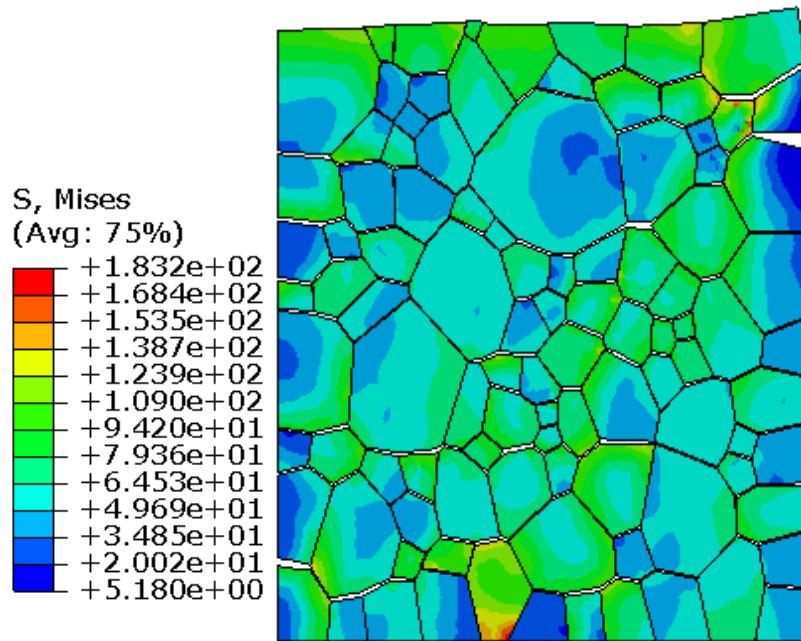


- Strong stress redistribution: the 'hard' phases withstand more load with the increased time. Stress concentration near the triple junctions and grain boundaries is caused by the grain boundary activities and the mismatch between these two phases. Accumulated strain is observed, especially in the soft grains.

Creep Rupture Behavior in ICHAZ: Case I, Time=813,629 s

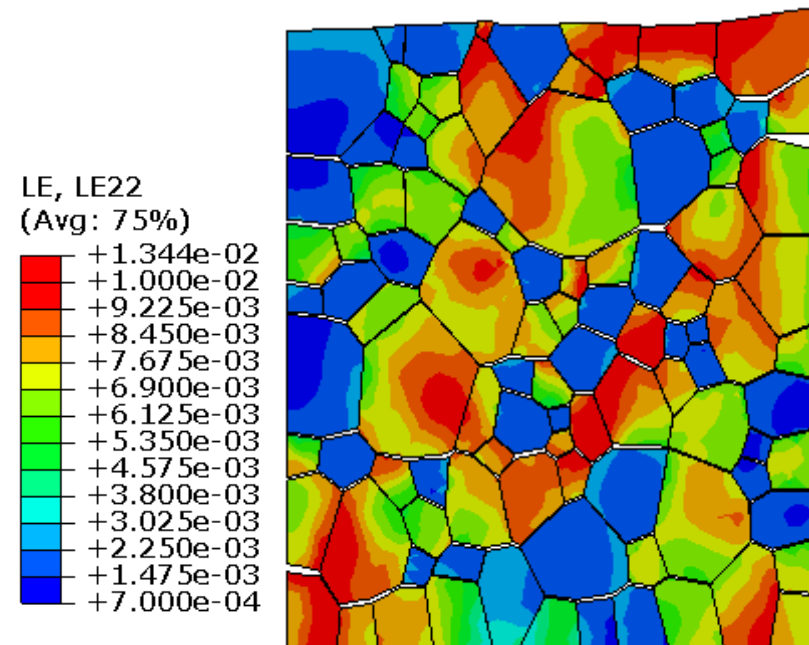


- Stress



- Strain

Case I: $\dot{\epsilon}_B = 10\dot{\epsilon}_A = 1.337 \times 10^{-8} s^{-1}$

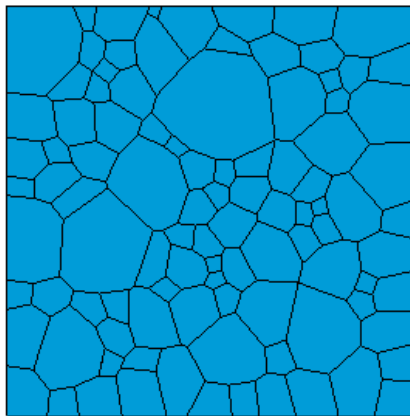
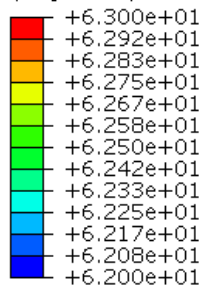


- Stress concentration disappears with the cavity nucleation, growth and formation of microcracks on the grain boundaries.

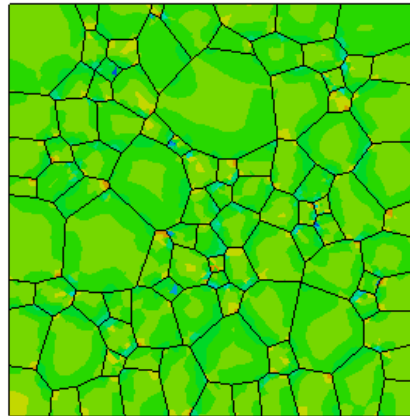
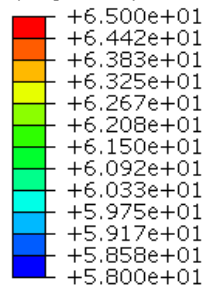
Creep Rupture Behavior in ICHAZ: Case III (same creep rate)

Stress

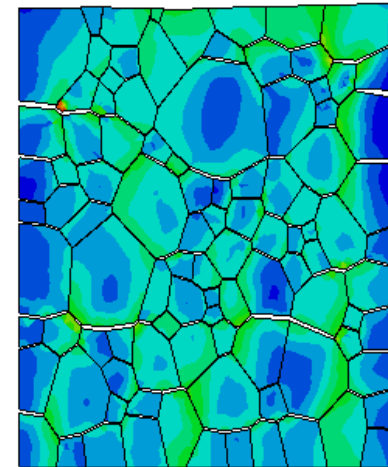
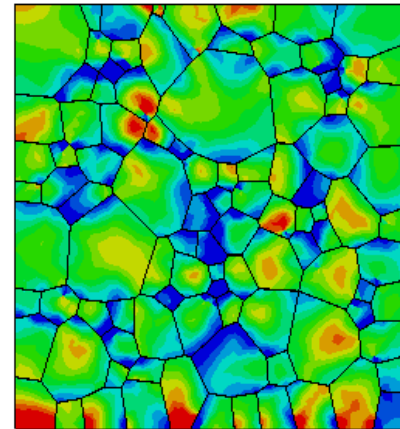
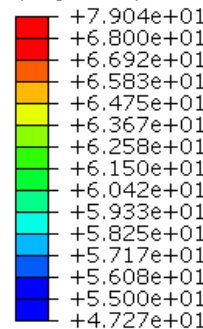
S, Mises
(Avg: 75%)



S, Mises
(Avg: 75%)

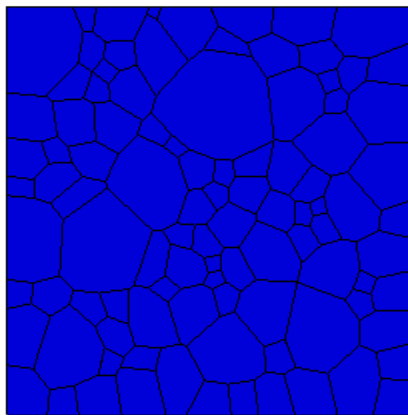
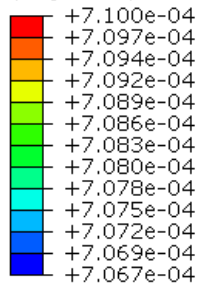


S, Mises
(Avg: 75%)

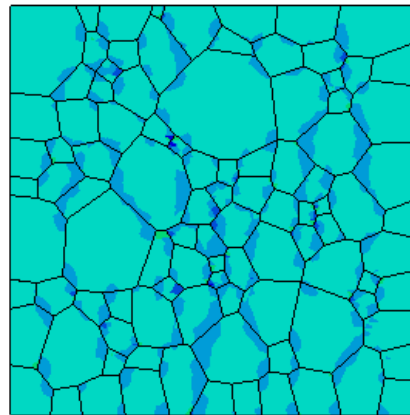
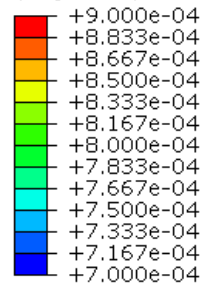


Strain

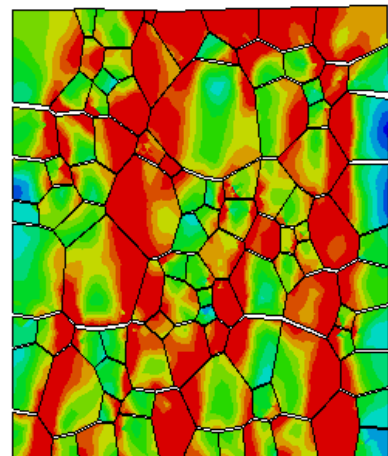
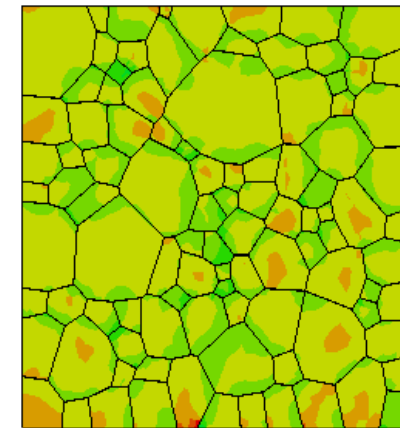
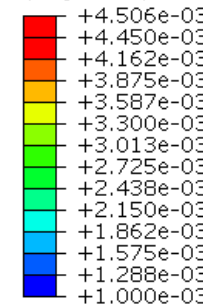
LE, LE22
(Avg: 75%)



LE, LE22
(Avg: 75%)



LE, LE22
(Avg: 75%)



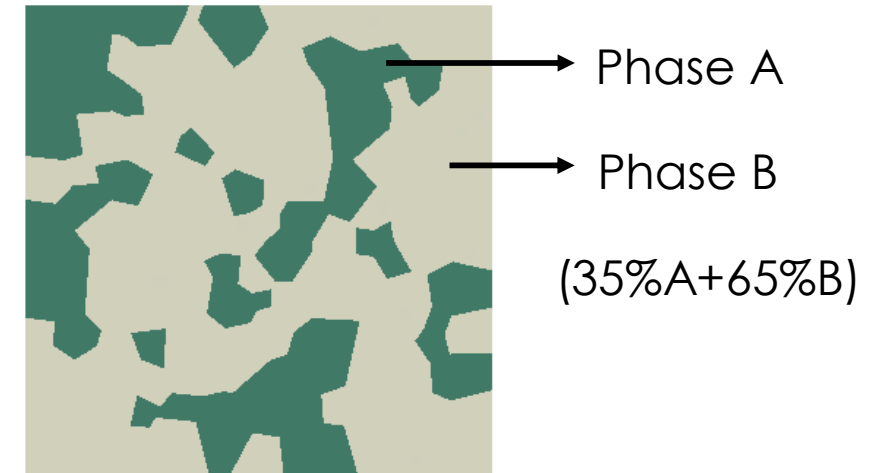
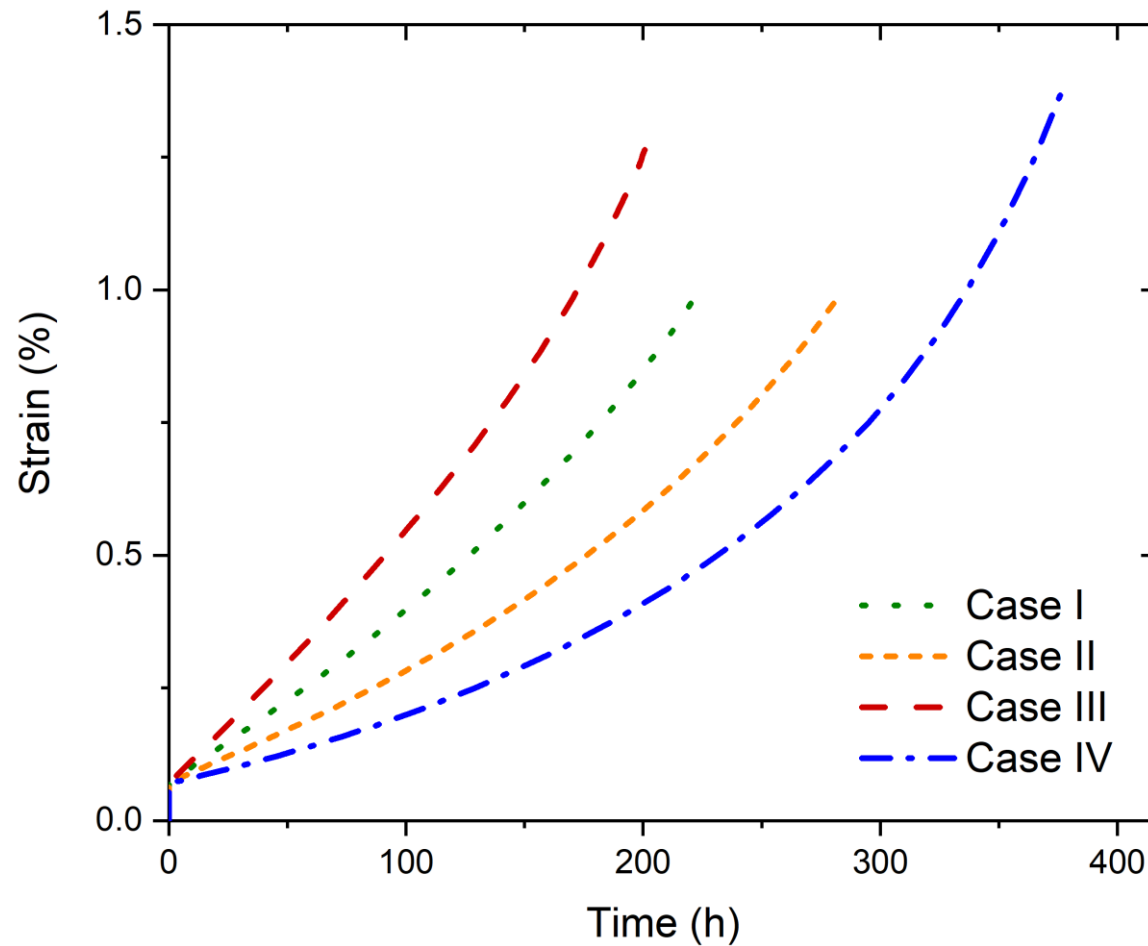
Time=1s

Time=4433s

Time=2.363e5 s

Time=7.222e5 s

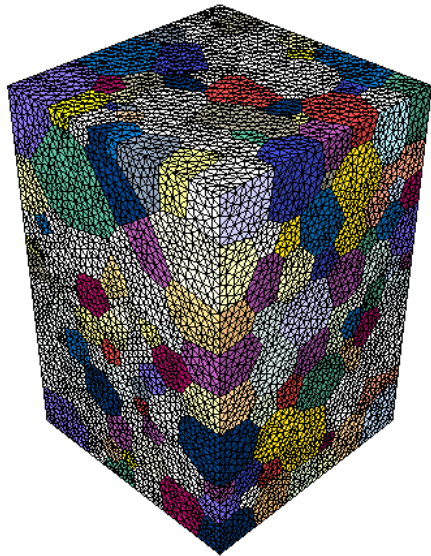
Creep Rupture Behavior in ICHAZ with Two Phases



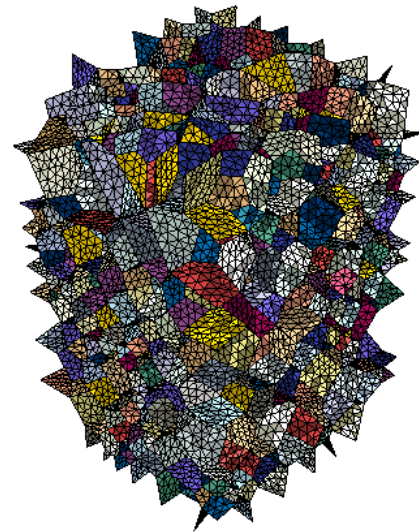
- Case I: $\dot{\epsilon}_B = 10\dot{\epsilon}_A = 1.337 \times 10^{-8} s^{-1}$
- Case II: $\dot{\epsilon}_A = 10\dot{\epsilon}_B = 1.337 \times 10^{-8} s^{-1}$
- Case III: $\dot{\epsilon}_A = \dot{\epsilon}_B = 1.337 \times 10^{-8} s^{-1}$
- Case IV: $\dot{\epsilon}_A = 10\dot{\epsilon}_B = 1.337 \times 10^{-9} s^{-1}$

Three Dimensional Model

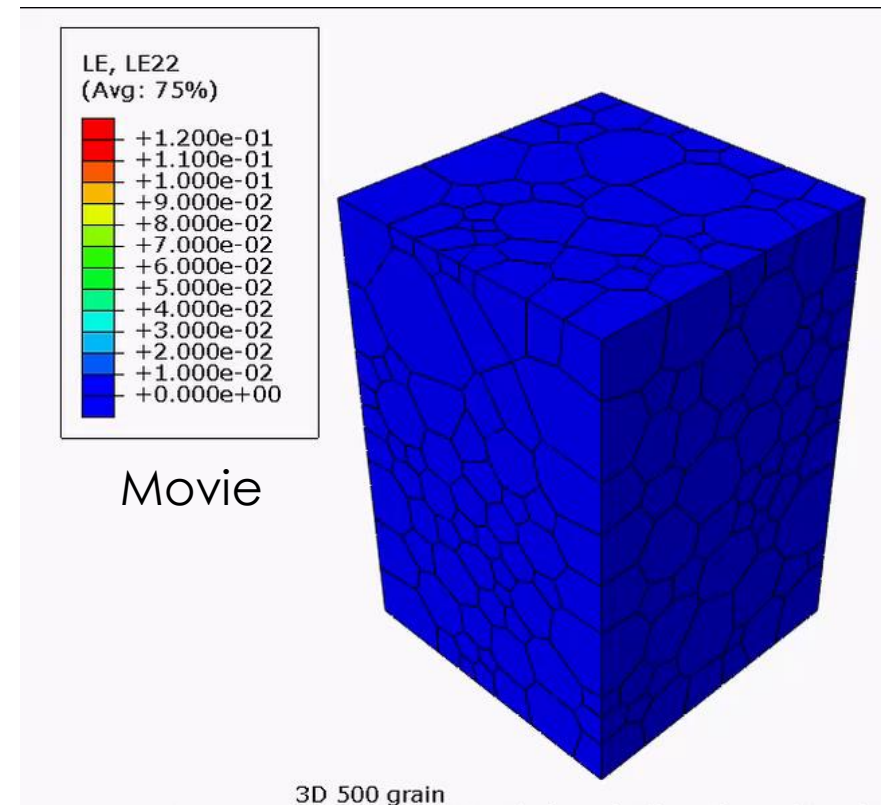
- To obtain more realistic localized and macroscopic deformation of the critical subregions in the weldment.



Model: 500 grains
~ 600,000 elements



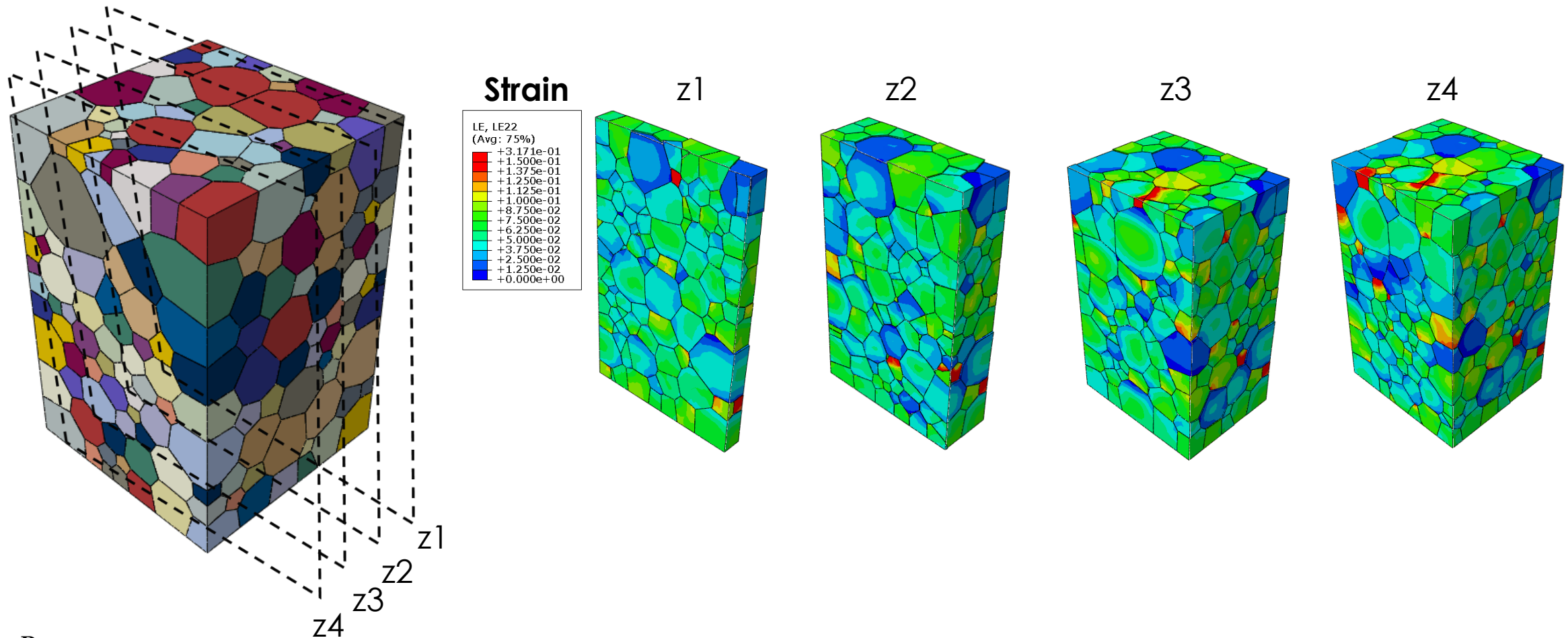
Grain boundary
Cohesive element



Strain evolution

Three Dimensional Model

- Inner strain distribution



Summary

- A new experiment approach, involving high-temperature creep testing, in-situ DIC measurement, advanced microscopy characterization, and standardized metallurgical analysis, has been developed to investigate creep performance of the CSEF steel welds.
- Localized creep deformation can be quantified by the specially-built DIC, to evaluate creep strength degradation in the CSEF steel welds.
 - The newly formed martensite in ICHAZ during welding has profound influence on the localized creep deformation.

Summary

- Demonstrated an engineering modeling approach (Level 1 model) for weld creep performance prediction based on the local DIC experimental data.
 - Potential for weld process innovation to improve weld creep performance
- Established ICWE modeling framework (Level 2) to simulate effects of key microstructure features and operating conditions (temperature and stress)
 - Capable of predicting creep rapture life of base metal and welds in literature
 - Demonstrated the feasibility of a micromechanics RVE model to provide microstructure informed constitutive relation for macroscopic weld structure performance prediction.

On-Going Work

- Additional experiments with varying key microstructure constituents in the HAZ of P91 weld to provide needed parameters to validate the model and make it applicable to specific CSEF materials and welds.
- Refine/fine tune the modeling approach to better connect microscopic RVE and macroscopic models
- Port the ICWE code to high performance computers (HPC) for realistic prediction of industry applications

Thank you!

ORNL is managed by UT-Battelle, LLC for the US Department of Energy

Key Milestones

- FY2015
 - Improve and standardize the ORNL weld creep test procedure and demonstrate its effectiveness to quantify the non-uniform creep deformation behavior in P91 weldments
- FY2016
 - Complete first stage of microstructural model with consideration of martensite/precipitates evolution and interaction
 - Develop a weld creep performance model using experimental determined creep parameters (Level 1)
- FY2017
 - Complete integration of microstructure model with RVE model (Level II)
- FY2018
 - Demonstrate the model developed in this project for creep life prediction
 - Report on the feasibility and potential of big data and deep learning method for creep life prediction of weldments
- FY2019
 - Complete integration of microscopic RVE with evolving microstructure features and macroscopic models for component level predictions (March 2019)
 - Port the ICWE code to high performance computers (HPC) for realistic prediction of industry applications (June 2019)
 - Complete purposely designed experiments with varying microstructures to support and validate the ICWE model (Sept. 2019)

“As-Received” Grade 91 base metal (Plate)

- Heat number: 30176
- Solid processing: hot forging, hot rolling
- Heat treatment:

Normalizing: 1050 °C-1 hour-AC, Tempering: 760 °C-2 hours-AC

Chemical composition (wt. %)									
C	Mn	P	S	Si	Ni	Cr	Mo	V	Nb
0.061	0.37	0.01	0.003	0.11	0.09	8.61	0.89	0.209	0.072
Ti	Co	Cu	Al	B	W	As	Sn	Zr	N
0.004	0.01	0.04	0.007	<0.09	<0.01	0.001	<0.001	<0.001	0.055

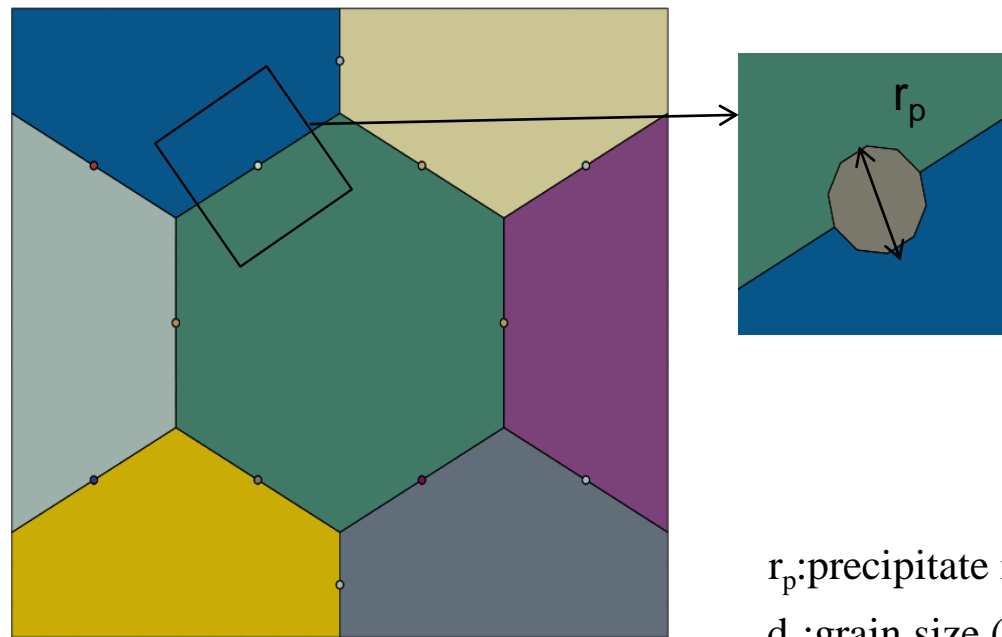
Material parameters

Parameter	Value
Atomic volume Ω	$1.18 \times 10^{-29} \text{m}^3$
Melting temperature T_M	1800K
Burgers vector b	$2.48 \times 10^{-10} \text{m}$
Young's modulus E_0	223GPa
Poisson's ratio ν	0.3
Grain boundary diffusion pre-exponent D_{0gb}	$0.0044 \text{m}^2/\text{s}$
Grain boundary diffusion activation energy Q_{gb}	174 KJ/mole
Coble creep coefficient A_{coble}	8.637×10^{-4}
Lattice diffusion pre-exponent D_{0l}	$0.021 \text{m}^2/\text{s}$
Lattice diffusion activation energy Q_l	500 KJ/mole
Dislocation creep coefficient A_{dis}	6.0×10^{24}
Stress exponent	8
Grain boundary sliding pre-exponent η_0	40 m/s
Average grain size in FGHAZ d	$1 \mu\text{m}$
Average grain size in the other zones d	$5 \mu\text{m}$

RVE Model for Carbide/Precipitate on Grain Boundary

- Explicitly determine the roles of carbides/precipitates on grain boundary deformation and failure

Unit cell model



r_p : precipitate radius
 d_g : grain size (5 microns)